Design Trade Study for High Altitude Payload Delivery UAV's

A thesis submitted in fulfillment of the requirements

for the degree of Master of Technology

by

Balachandar D

17101016

DEPARTMENT OF AEROSPACE ENGINEERING

INDIAN INSTITUTE OF TECHNOLOGY KANPUR

June 2019

Certificate

It is certified that the work contained in this thesis entitled "**Design Trade Study for High Altitude Payload Delivery UAV's**", by **Balachandar D** (Roll No. **17101016**), has been carried out under our supervision for the partial fulfillment of masters degree in the Department of Aerospace Engineering, IIT Kanpur and that it has not been submitted elsewhere for a degree.

Signature of Supervisor

Dr. Mangal Kothari

Professor

Department of Aerospace Engineering

Indian Institute of Technology Kanpur

June 8, 2019

Signature of Co-Supervisor

Dr. Abhishek

Professor

Department of Aerospace Engineering

Indian Institute of Technology Kanpur

STATEMENT OF THESIS PREPARATION

1. Thesis title : **DESIGN TRADE STUDY FOR HIGH ALTITUDE PAYLOAD DELIVERY UAVs.**
2. Degree for which the thesis is submitted : **M.TECH.**
3. Thesis Guide was referred to for preparing the thesis.
4. Specifications regarding thesis format have been closely followed.
5. The contents of the thesis have been organized based on the guidelines.
6. The content of the thesis has been prepared without resorting to plagiarism.
7. All the sources have been cited appropriately.
8. This thesis has not been submitted elsewhere for a degree.

(Signature of the student)

Name: BALACHANDAR D

Roll no: 17101016

Department/IDP: AEROSPACE ENGINEERING

Abstract

Name of the student: **Balachandar D** Roll No: **17101016**

Degree for which submitted: **M.Tech.** Department: **Aerospace Engineering**

Thesis title: **Design Trade Study for High Altitude Payload Delivery UAV's**

Thesis supervisor: **Dr. Mangal Kothari**

Thesis Co-supervisor: **Dr. Abhishek**

Month and year of thesis submission: **June 2019**

Lightweight autonomous Rotary Wing Unmanned Aerial Vehicles (RWUAV) are preferred for high altitude missions where human's participation becomes challenging. These high altitude missions may include payload delivery, surveillance, search, and rescue. Till now, such RWUAVs are not available for these missions. Experience in the design of rotary wing UAVs for such missions is lacking because of the absence of formal methodology for preliminary sizing and design of such RWUAVs. This thesis, explores the feasibility of design of a conventional helicopter and a multirotor for a high altitude payload delivery mission. Two separate designs are explored for the conventional helicopter, one with fuel powered and another with electric powered while the multirotor design is all electric. The mission requirement is to take off with 20kg payload at an altitude of 5500m above mean sea level, cruise to the target for delivery and cruise back to the departure point for landing. A method to study the effect of critical design parameters based on the mission requirement is developed. Existing empirical methods from different literature are explored to estimate group weights of various components. Forward flight power is calculated using Momentum Theory while hover at out of ground effect (HOGE) power is computed using Blade Element Momentum Theory. A trade study of design parameters using Carpet plots is done

to identify baseline design parameters for all the three vehicles. Preliminary design of Rotary wing UAV is an excellent example of a complex environment where there are several interdependent design variables and objectives. Hence a Multi-Objective Optimization is carried out using a Genetic Algorithm to obtain optimal designs. The designs proposed is a compromise between maximum takeoff weight and overall power consumption. This thesis shows the feasibility of developing a rotary wing UAV for missions at high altitudes and this will be a foundation for the detailed design.

Acknowledgements

I would like to express my sincerest gratitude to my thesis supervisor, **Dr. Mangal Kothari** for allowing me to work under him and for his invaluable guidance and suggestions. He gave me full freedom to solve the problem and also provided me with a peaceful atmosphere to work in IGCL lab. I would also like to extend my sincere gratitude to my thesis co-supervisor, **Dr. Abhishek** for his guidance and patiently showing me the path whenever I get stuck. He provided me a great degree of freedom and flexibility in my research. I also thank him for teaching subjects "Helicopter Theory – Dynamics and Aeroelasticity" and "Preliminary Design of Helicopters" which helped me to improve my technical skills to a great extent. Without their valuable assistance, this work would not have been completed.

I would like to thank my friends Karthikeyan and Govindasamy for being with me in my good and bad days without whom I would not have come this far. I would like to thank my friends Akhshaya, Keesanth, Navya, Vijay, Madhu, Booma, Soori, Basab and Deep for constantly cheering me up in my hard days, giving me ideas whenever I get stuck with a problem and sharing my passion for traveling. I have learned a lot from them and without their support, spending two years on this campus would have been difficult.

I am thankful to those who gave me their valuable time and enthusiasm during these years. I would also like to thank my lab mates for their help and support and also for having wonderful discussions which improved my intellectual skills. I also thank Rahul Ramanujam for his advice and help in completing this work successfully.

I greatly indebted to Bhuvana, who became a part of my life and supported me in all my endeavors. Finally, I also thank my mother and brother for their love, care and allowing me to pursue my dreams despite all the problems they had faced without which this work would not have been possible.

- Balachandar D

Contents

List of Figures

List of Tables

Abbreviations

AMSL	**A**bove **M**ean **S**ea **L**evel
BET	**B**lade **E**lement **T**heory
BEMT	**B**lade **E**lement **M**omentum **T**heory
BLDC	**B**rush**L**ess **D**irect **C**urrent
CFD	**C**omputational **F**luid **D**ynamics
ESC	**E**lectronic **S**peed **C**ontroller
GTOW	**G**ross **T**ake **O**ff **W**eight
HOGE	**H**over **O**ut off **G**round **E**ffect
IGE	**I**n **G**round **E**ffect
IRA	**I**ndian **R**eference **A**tmosphere
UAV	**U**nmanned **A**erial **V**ehicle
RWUAV	**R**otary **W**ing **U**nmanned **A**erial **V**ehicle
VTOL	**V**ertical **T**ake **O**ff and **L**anding
ZHI	**Z**ero **H**orsepower **I**ntercept

Symbols

a	speed of sound
A_{mr}, A_{tr}	main rotor and tail rotor disk area
AR_{mr}, AR_{tr}	main rotor and tail rotor aspect ratio
AR_{ht}, AR_{vt}	aspect ratio of horizontal and vertical tail
N_b	number of main rotor and tail rotor blades
B	tip loss factor
c	local blade chord
C	Capacity of the battery
C_L	coefficient of lift
$C_{L\alpha}$	lift curve slope
C_{d0}	drag coefficient
dL , dD	Incremental lift and drag components
DL	disk loading
f	equivalent flat area
ffr	fuel flow rate
F	prandtl's tip loss correction factor
HP_{mr}, HP_{tr}	main rotor and tail rotor drive system horsepower
I_{max}	maximum current
K_v	motor speed constant
L	distance between main rotor shaft and tail rotor shaft
L_f	length of the fuselage
$\dot{m}$	mass flow rate
n_{ult}	ultimate load factor

NOR	number of rotors in a multirotor
dP	incremental rotor power
P_{alt}	power available at an altitude
P_{msl}	power available at mean sea level
P_{mr}, P_{tr}	main rotor and tail rotor power
P_{losses}	power losses
P_{acc}	accessories power
P_{HOGE}	hovering out of ground effect power of the vehicle
P_0	parasitic power
P_p	profile power
P_i	induced power
P_{total}	total power
P_{hp}	zero horsepower increment
dQ	Incremental rotor torque
Q_{mr}	main rotor torque
R_{mr}, R_{tr}	main rotor and tail rotor radius
S	number of battery cells connected in series
S_{ht}, S_{vt}	Surface area of horizontal and vertical tail
dT	Incremental rotor thrust
T_{mr}, T_{tr}	main rotor and tail rotor thrust
U_T	in-plane velocity
U_P	out-of-plane velocity
U_R	radial velocity
U	resultant velocity
v_i	induced velocity
$V_{tip_{mr}}$, $V_{tip_{tr}}$	main rotor and tail rotor tip speed
W_{mrb}	main rotor blade weight
W_{hh}	hub and hinge assembly weight
W_{fuse}	fuselage weight
W_{tr}	tail rotor group weight
W_{lg}	landing gear weight

W_{ht}, W_{vt}	horizontal and vertical tail weight
$W_{control}$	controls weight
W_{elec}	electrical equipment weight
$W_{trans_{mr}}$, $W_{trans_{mr}}$	main rotor and tail rotor transmission weight
W_{empty}	empty weight
$W_{payload}$	payload weight
W_{fuel}	fuel weight
W_{motor}	motor weight
W_{esc}	electronic speed controller weight
W_{prop}	propeller weight
W_{wiring}	wiring weight
$W_{airframe}$	airframe weight
$W_{battery}$	battery weight
W_{gross}	gross weight
y	dimensional radial distance of blade element
σ_{den}	density ratio
σ_{mr}, σ_{tr}	main rotor and tail rotor solidity
θ_{temp}	temperature ratio
θ	pitch angle of blade element
$\theta_{coll_{mr}}$, $\theta_{coll_{tr}}$	main rotor and tail rotor blade collective pitch angle
ρ	density
α	effective angle of attack
ϕ	inflow angle
Ω	rotational speed of the rotor
λ	inflow ratio
δ	pressure ratio

To my Father...

Chapter 1

Introduction

Unmanned Aerial Vehicle (UAV) also known as a drone, is an autonomous aircraft without a pilot onboard. In recent years, UAV's are most commonly used for many applications like surveillance, agriculture, payload delivery, and inspection of critical infrastructures. While fixed-wing UAVs are also used, Rotary Wing Unmanned Aerial Vehicles (RWUAV) which includes helicopters and multi-rotors are mostly preferred for these applications because of its Vertical Takeoff and Landing (VTOL) capability. This capability allows RWUAV to take off and land in any terrain without a long runway. In the last ten years, the design and development of such small size RWUAVs have increased because of its advantage over fixed-wing UAVs in many applications. Payload delivery is one such application where RWUAVs are preferred over fixed-wing UAV for their VTOL capability.

Even though there are many RWUAV's designed for sea level applications, evaluation of existing RWUAV's[18], shows that none of them can perform missions significantly at high altitudes. No RWUAV that can deliver a payload at altitude more than 5000 m AMSL exists. The new field of applications such as research in high mountain regions, search and rescue of mountain climbers, surveillance and payload delivery for military command post located at high altitude areas would open up if the flight envelope of these RWUAVs is expanded. The objective of this thesis is to explore RWUAV configurations and design a

RWUAV that can deliver a payload of 20kg at an altitude of 5500m AMSL. Development of this RWUAV for payload delivery in high altitude areas will enable continuous logistic supply leading to the operational efficiency of the troops operating at high altitude areas.

Experience in designing a RWUAV for high altitude applications is lacking, because there are many developed full-scale helicopters available in the literature, but there are not many vehicles within class 1 category[18], particularly for high altitudes. Different versions of rotary vehicle design programs used for full-scale helicopters may not apply to class 1 weight category RWUAVs. Therefore a formal methodology has to be developed to design such RWUAV. The design process starts with the conceptual and preliminary design phase where initial RWUAV configuration and sizing has to be done in a shorter time and reduced cost. Hence preliminary design phase uses theoretical estimation values and appropriate analysis tool for the faster design. This thesis focuses on design trade study and preliminary design of RWUAVs for high altitude payload delivery missions. Design trade study helps to investigate the influence of critical design parameters and obtain an optimal design solution from a mission-based point of view while preliminary design helps in sizing the concept.

Since the engine and battery performance degrades drastically in high altitudes, a highly efficient vehicle has to be designed. A conventional helicopter is the most efficient VTOL capable system out off all the UAVs in the world. Moreover, the vehicle also should have easy maintenance, use off-the-shelf parts, and be easily deployable. Multirotor's are mechanically simple, easy to build using off-the-shelf parts and are easy to maintain and transport. Hence, in this thesis, conventional helicopter with tail rotor configuration and multirotor designs are explored for the mission requirements given in Section 1.1.

1.1 Mission Requirements

Understanding the mission requirements is the first step in any design process. The objective of the vehicle is to perform a payload delivery mission at high altitude region in Indian Reference Atmosphere (IRA) conditions.

TABLE 1.1: Mission profile for conventional helciopter configuration

Description	**Altitude(km)**	**Flight**
Warm up/Takeoff	5.5	3 min
Cruise at Maximum Range Velocity	5.5	100 km
Reserve Cruise at Maximum Endurance Velocity	5.5	15 min
Approach/Landing	5.5	3 min

It should have Vertical Takeoff and Landing (VTOL) capability to land in snow and locations that do not have flat terrain or conventional runway. The vehicle should be autonomous and be able to launch multiple times a day with less maintenance action. The vehicle should be able to carry and deliver a 20kg payload within a minimum range of 100km. In this thesis, both electric and fuel power source are used for RWUAV design. Mission profile considered for a conventional helicopter configuration is given in Table 1.1. The vehicle has to takeoff at an altitude of 5500 m and cruise flight altitude is not more than 100ft above 5500 m. Hence for all the segment of the mission, altitude of 5500 m is considered. Due to the difference in the energy density of fuel and battery, a slightly different mission is considered for the multirotor vehicle and is given in Table 1.2.

TABLE 1.2: Mission profile for a multirotor configuration

Description	**Altitude(km)**	**Time(min)**
Warmup/Takeoff	5.5	3
Crusie at Maximum Range Velocity	5.5	24
Approach/Landing	5.5	3

1.2 Literature Survey

There are many preliminary design process concerning full-scale conventional rotorcraft, but design process for class-1 category RWUAV's used in industries and research institutes

are not commercial and have limited availability. Some of the works that are studied to develop a design process for a conventional helicopter are given below,

- [14] explains three approaches to preliminary design problem of a helicopter. The study of relationships among design parameters and its effect on helicopter performance called parametric analysis is explained in helicopter design handbook [10].
- Preliminary design process of a conventional helicopter is explained in the book "helicopter performance, stability, and control" by Prouty [23].
- Weight estimation formulas for different weight class of helicopters are given in [24][25][16][20].
- Weight estimation and preliminary design of helicopters using CFD and CAD designs are explained in [2][11].
- Ananth's approach[13] explains preliminary sizing of a helicopter using a genetic algorithm.
- A. Barth et al. shows the conceptual study of RWUAV for extreme altitudes using parametric analysis[6][5].

FIGURE 1.1: Schiebel Camcopter-S100 [1]

FIGURE 1.2: Aeroscout Scout-B330 [2]

Some of the commercially available RWUAVs that are of same weight class category of the current design is given in Figure 1.1 and 1.2. The baseline design parameters are

[1] https://schiebel.net/products/camcopter-s-100/
[2] https://www.aeroscout.ch/index.php/scout-uav-helicopters/scout-uav-helicopters-2/

decided based on these RWUAVs and design trends of existing RWUAVs given in [18]. Design trade study is done to investigate the effect of critical design parameters on the RWUAVs performance, and multi-objective optimization is carried out using a genetic algorithm to find an optimal design based on the mission requirement. In this thesis, not only a fuel powered RWUAV but all-electric RWUAV design is also explored. Lithium-Ion batteries are most commonly used in electric vehicles and solar aircrafts. The energy density of Lithium-Ion batteries depends on the electrodes and anodes used. [28] explains how Lithium Ion batteries are used efficiently to power a complete solar-powered aircraft. Full-scale helicopters that are converted from fuel-powered to all-electric is given in Figure 1.3 and 1.4. Battery performance degrades in a lower temperature, [6] shows how an insulation pack can be used to preserve the battery performance in higher altitudes.

FIGURE 1.3: OC Helicopters-Electric R22 [3]

FIGURE 1.4: Sikorsky Firefly [4]

Multirotors are the most popular aerial vehicles that are mechanically simple and controlled automatically or by a human. For this reason, multi-rotors are being used in many applications. Works that are studied to develop a design process of a multirotor are given below,

- Windtunnel and hover performance test results for five different multirotors are presented in [9], which determine forces, moments and electric power that can be used to develop analytical and numerical models for design and analysis of multirotors.

[3] https://www.foxtechfpv.com/gaia-190mp-heavy-lift-drone.html
[4] https://www.foxtechfpv.com/gaia-190mp-heavy-lift-drone.html

- Dmitry et al.[7], Abatis et al. [3] and Winslow et al.[27] describes the sizing of electric motor propulsion system using parametric analysis of multirotor components.

While these methods allow optimizing the propulsion system based on the mission requirements and vehicle parameters, no tool that allows designing a multirotor based on the mission exists. The most known online multirotor sizing and performance tool is ecalc[5], which allows calculating the performance characteristics based on the drive components. The goal of this thesis is to develop a design process for multirotor sizing that uses the parametric techniques for estimating the physical and electrical properties of the multirotor components. Some of the commercially available multirotor's that are close to the same weight class category and payload carrying ability of the current design are given in Figure 1.5 and 1.6.

FIGURE 1.5: Vulcan Airlift [6]

FIGURE 1.6: GAIA 190MP [7]

1.3 Organization of Thesis

The thesis is divided into five chapters, the outline of which is as follows:

Chapter 2 presents the design of a fuel-powered RWUAV. It discusses the weight estimation formulas, the power calculation using Blade Element Momentum Theory and design parameters trade study. It also presents the final design from Pareto optimal solutions using multi-objective optimization technique based on genetic algorithm.

[5]https://www.ecalc.ch/xcoptercalc.php
[6]http://vulcanuav.com/aircraft/
[7]https://www.foxtechfpv.com/gaia-190mp-heavy-lift-drone.html

Chapter 3 presents the design of an electric powered multi-rotor. It presents the design methodology used for this study, power calculation of fixed pitch propeller using Blade Element Momentum Theory and results including the carpet plots and the final design.

Chapter 4 presents the design of an electric powered RWUAV. It explains the battery and electric motor selection for the RWUAV. Design parameters study with the final design is presented.

Chapter 5 summarizes the thesis and discusses its future scope.

Chapter 2

Fuel Powered Conventional Helicopter

This chapter presents the design trade study and preliminary sizing of a fuel powered RWUAV. The objective of this process is to design a light, efficient, and easily maintainable RWUAV that satisfies all the mission requirements given in section 1.1. First, the engine selected for this RWUAV design is discussed. Then, Momentum Theory and Blade Element Momentum Theory are explained. These methods are used to calculate the power required during hover and forward flight of the RWUAV. Then, component weight estimation formulas from different sizing methods that are used to size the RWUAV are given. Next, the methodology forf the design trade study is illustrated. Finally, a multi-objective optimization using genetic algorithm is explained and the performance of the optimal design at 5500 m AMSL is shown.

2.1 Engine Selection

One of the mission requirements is to use a Wankel engine indigenously developed at the National Aerospace Laboratories for this current RWUAV design. A 65 hp single rotor,

liquid cooled engine was designed, developed and the 1st Prototype was successfully tested [22]. The Wankel engine is an internal combustion engine that is found increasingly used in UAVs where their compact size and quiet running is important. The Wankel engine is chosen because of its high power to weight ratio. The Wankel engine is also smaller in size when compared to a piston engine of the same class.

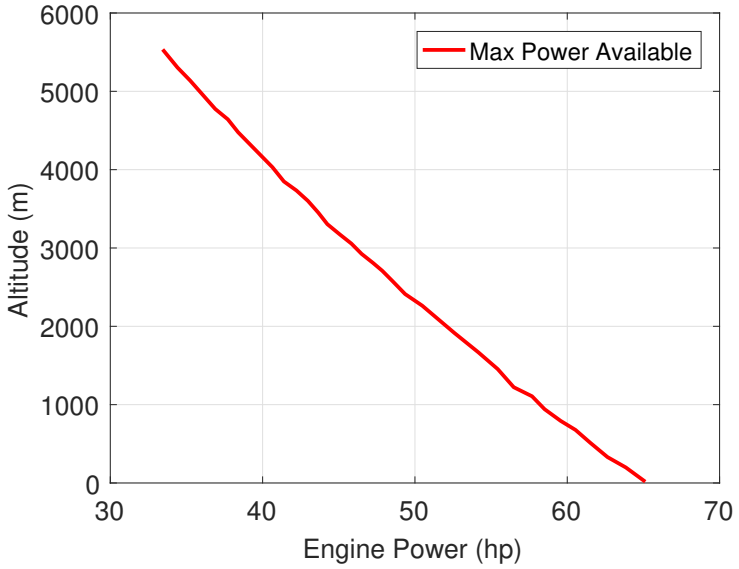

FIGURE 2.1: Wankel Engine Performance[22].

Figure 2.1 shows the maximum power available of the Wankel engine with respect to altitude. The continuous power of Wankel engine at sea level is 55 hp while the continuous power available at an altitude of 5500 m is not available. For a nonsupercharged reciprocating engine, power curves vary almost linearly with density ratio, σ. Assuming reciprocating and Wankel engine behaves similarly, power available at any altitude can be calculated by a normal approximation given in the Equation 2.1 [20]. And also from [19], it is observed that at an altitude of 15000ft Wankel engine's power drops by a factor of 1.7.

$$P_{alt} = P_{msl}\left(\frac{1.133\sigma - 0.133}{\sqrt{\theta}}\right) \tag{2.1}$$

Where, P_{alt} is the power available at an altitude and P_{msl} is the power available at mean sea level conditions.

From the Equation 2.1, continuous power available from the Wankel engine at 5500 m is found to be 30 hp. This is one of the major constraints in this design since this decides the hovering capability of the RWUAV at that altitude. The dry weight of the considered Wankel engine is 35.6 kg. The weight of the other propulsion subsystem components like engine ECU, exhaust, oil tank, and throttle body is around 11 kg.

2.2 Power Calculation

An important aspect of designing a RWUAV is the calculation of accurate power, torque, and collective pitch angle to hover based on rotor geometry and the required thrust. The operational power with desired flight time will give the required energy capacity, which in terms determine the fuel weight. The design is also based on the hover out of ground effect (HOGE) power at the mission altitude constrained by the engine performance. The accurate rotor performance can be studied using CFD based on free wake methods. In these methods, rotor performance is predicted by calculating the vortical wake structure, which is time-consuming and has high computational cost. For preliminary design, it is preferable to use some simple methods to analyze the rotor with lower accuracy and also lower computational cost. The rotor aerodynamics is different for each flight conditions like hovering, climb, descent, or forward flight. Hence each flight conditions has to be modeled using different methods. Some of the methods used in this thesis are Momentum Theory, Blade Element Theory, and Blade Element Momentum Theory, which is a combination of the previous two. Below sections explain how BEMT and Momentum Theory are used to calculate the power required by the RWUAV during hovering and forward flight conditions respectively.

2.2.1 Hover Performance

Momentum theory, a simple approach is given by Rankine(1865), Froude(1878) and Glauert(1935). This approach helps us to perform the first level of analysis of the rotor performance, but without actually considering what is happening locally at each blade section. In this theory, the rotor can be assumed as an infinitesimally thin actuator disk over which a pressure difference exists. It is assumed that flow through the rotor is one-dimensional, quasi-steady, incompressible, and inviscid. Figure 2.2 shows the flow model of the rotor during the hovering condition. The conservation laws of mass, momentum, and energy are applied to the control volume given in Figure 2.2.

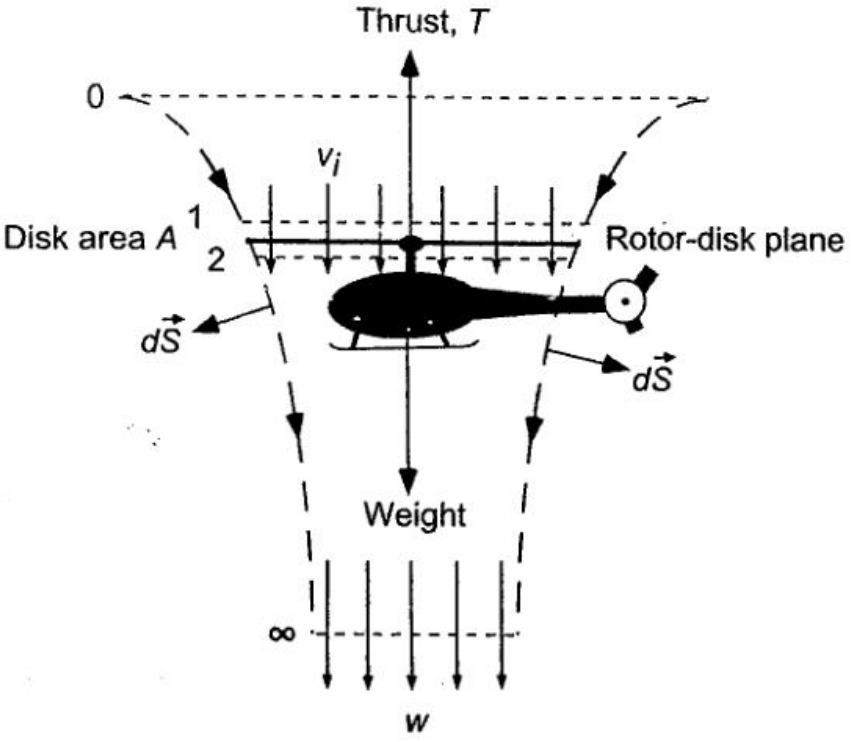

FIGURE 2.2: Flow model of a rotor in hovering flight[20].

From the conservation of mass, the mass flow rate $\dot{m}$ in the control volume is

$$\dot{m} = \rho A v_i \tag{2.2}$$

where v_i is the induced velocity imparted to the air by the rotor disk, and A is the rotor disk area.

From the conservation of momentum, the force on the rotor is the net time rate of change of momentum of air out of the control volume.

$$T = \dot{m}w \tag{2.3}$$

Where, w is the velocity of the air far down from the rotor.

Conservation of energy gives the relationship between the work done on the rotor and the gain in energy per unit time. Power consumed by the rotor is given by

$$Tv_i = \frac{1}{2}\dot{m}w^2 \tag{2.4}$$

From Equations 2.3 and 2.4 it is clear that the velocity at far wake is twice the induced velocity.

$$w = 2v_i \tag{2.5}$$

Thrust and power of the rotor can be written in terms of induced velocity as in Equations 2.6 and 2.7.

$$T = \dot{m}w = 2\rho A v_i^2 \tag{2.6}$$

Since the flow assumed is inviscid and incompressible, ideal power given in Equation 2.7 is entirely induced.

$$P = Tv_i = 2\rho A v_i^3 \tag{2.7}$$

Blade Element Theory considers the geometrical shape of the blade like blade twist, planform and perhaps the airfoil shape to find the performance of the rotor, unlike momentum theory. BET assumes that several blades form a rotor and each blade is divided into multiple elements, and each blade element acts as a quasi 2D aerofoil to produce aerodynamic forces and moments. Prandtl's tip loss factor is applied to account for three-dimensional effects. The sectional forces are integrated throughout the rotor to compute

thrust, torque, and power.

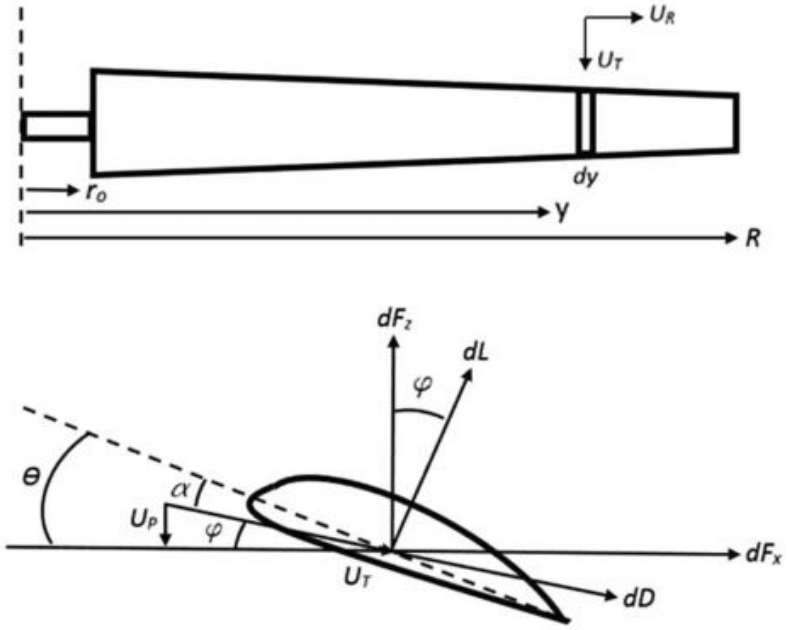

FIGURE 2.3: Schematic of a blade element and components of velocity experienced by it[20].

Figure 2.3 shows the rotor blade element, velocities, and aerodynamic forces experienced by it. There are three velocity components U_T, U_P and U_R. U_T is the in-plane/tangential velocity component that is parallel to the rotor disk produced from the blade rotation. U_P is the out of plane/perpendicular velocity component acting normal to the rotor disk due to induced inflow. U_R is the radial component along the blade span that does not contribute to lift generation but will affect the drag on the blade during forward flight. Hence for hover performance, U_R is ignored. The resultant velocity (U) acting on the blade is given by,

$$U = \sqrt{U_T^2 + U_P^2} \tag{2.8}$$

$$U_T = \Omega y; \qquad U_P = v_i; \tag{2.9}$$

Where Ω is the rotational speed of the rotor, y is the dimensional radial distance of the

blade element. Because of the velocity induced by the rotor and its wake, the relative flow velocity vector is modified, which also alters the local angle of attack of each blade element. The inflow angle and effective angle of attack of the blade element is given by,

$$\phi = tan^{-1}\left(\frac{U_P}{U_T}\right) \tag{2.10}$$

$$\alpha = \theta - \phi \tag{2.11}$$

where θ is the pitch angle of the blade element.dL and dD, the resultant incremental lift and drag per unit span on this blade element are,

$$dL = \frac{1}{2}\sigma U^2 c C_l dy \tag{2.12}$$

$$dD = \frac{1}{2}\sigma U^2 c C_d dy \tag{2.13}$$

where c is the local blade chord, C_l and C_d are lift and drag coefficients. While lift and drag forces are with respect to resultant flow velocity, the forces that are parallel and perpendicular to the rotor disk are represented as,

$$dF_z = dLcos\phi - dDsin\phi \tag{2.14}$$

$$dF_x = dLsin\phi + dDcos\phi \tag{2.15}$$

In hover condition, the flow environment is axisymmetric and the forces and moments are independent of the blade azimuth angle. Therefore, the incremental thrust, torque, and power of the rotor can be represented as

$$dT = N_b dF_z \tag{2.16}$$

$$dQ = N_b dF_x y \tag{2.17}$$

$$dP = N_b dF_x \Omega y \tag{2.18}$$

where N_b is the number of blades in the rotor. The nondimensional quantities, inflow ratio and rotor solidity are written as,

$$\lambda = \frac{v_i}{\Omega y} = \phi r \tag{2.19}$$

$$\sigma = \frac{N_b c}{\pi R} \tag{2.20}$$

For a rectangular blade, solidity σ is the ratio of the rotor blade area to the rotor disk area. The method that uses equation 2.6 and 2.12 to calculate inflow distribution on the rotor is described below.

Blade Element Momentum Theory presented in [20] combines both the momentum theory and BET. Momentum theory assumes uniform inflow while BET assumes the inflow varies as a function of rotor radius. BEMT invokes the equivalence between the incremental thrust coefficients for an annulus of the rotor disk from both the methods to find the inflow characteristics of the rotor. BEMT also has the same assumptions as BET that the mutual effects between successive blade elements are not considered. Hence, this method has good validity except near the blade tips. A good approximation of the tip loss effect on the inflow distribution is made using Prandtl's function. Equation 2.21 and 2.22 represents the incremental thrust coefficients for an annulus of the rotor disk for momentum theory and BET respectively.

$$dC_T = 4F\lambda^2 r dr \tag{2.21}$$

$$dC_T = \frac{1}{2}\sigma C_{l_\alpha}\left(\theta r^2 - \lambda r\right) dr \tag{2.22}$$

where λ is the inflow ratio, σ is the solidity, r is the non-dimensional radial position and dr is the non-dimensional radial increment. Equating the above two equations will give,

$$4\lambda^2 r dr = \frac{1}{2}\sigma C_{l_\alpha}\left(\theta r^2 - \lambda r\right) dr \tag{2.23}$$

The inflow ratio for a specific radial location can be found by solving the quadratic equation arising from rearranging the equation 2.23. The inflow ratio is given by,

$$\lambda_i(r) = \frac{\sigma C_{l_\alpha}}{16F}\left(\sqrt{1+\frac{32F}{\sigma C_{l_\alpha}}\theta r}-1\right) \tag{2.24}$$

Where F is the Prandtl's tip loss correction factor given by

$$F = \left(\frac{2}{\pi}\right) cos^{-2}\left(exp\left(-f\right)\right) \tag{2.25}$$

Where f is given as a function of number of blades and the radial position of the blade element r, by

$$f = \frac{N_b}{2}\left(\frac{1-r}{r\phi}\right) \tag{2.26}$$

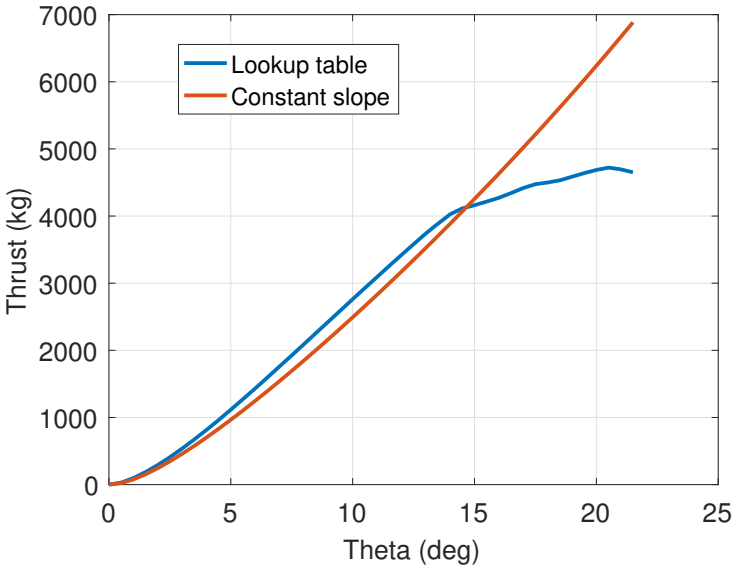

FIGURE 2.4: Comparison of Lift calculation methods.

From equation 2.24, inflow ratio cannot be solved immediately because λ is a function of F and F is again a function of λ. It is solved iteratively by calculating the initial inflow ratio using F=1 and then finding F from 2.25 and recalculating λ from the numerical solution to 2.24. Iteration continues until the error between the successive inflow values is below

a certain threshold. Finally, the aerodynamic forces and moments are calculated from equations 2.12 - 2.18 to estimate the performance of the rotor.

Usually, for preliminary analysis, a constant lift curve slope and drag coefficient is used to calculate forces and moments based on the local angle of attack experienced by the rotor section. In this work, accuracy in aerodynamic force calculation is improved by using a lookup table for C_L and C_D values. Figure.2.4 shows the comparison of BEMT thrust values using lookup table for C_L, C_D values and constant C_{L_α}. Look-up table includes C_L and C_D values of NACA0012 aerofoil for a different angle of attack and Mach number. The comparison shows that the stall effect is modeled when the lookup table is used to find aerodynamic coefficients.

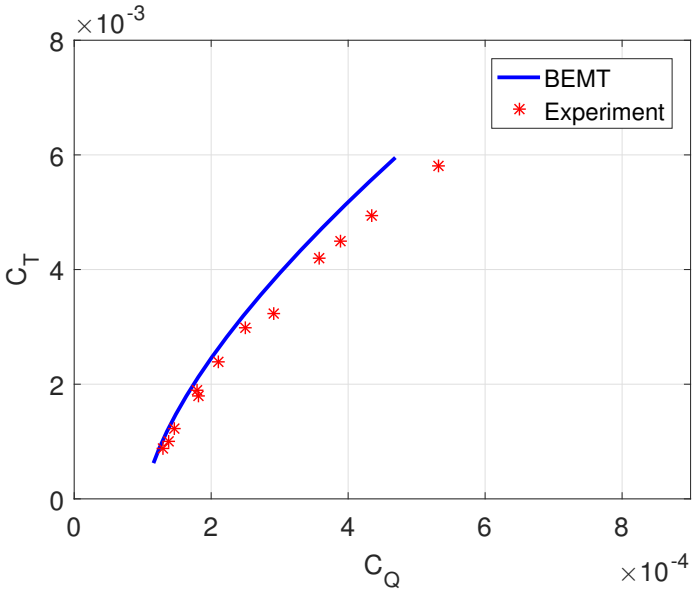

FIGURE 2.5: Experimental validation of BEMT calculation

BEMT method is validated with the experiment done by Harrington [15]. Figure.2.5 shows the comparison between BEMT calculation and experimental result for rotor2 configuration. Rotor radius is 3.81 ft, chord is 0.45 ft, and tipspeed is 262 ft/s. Since a different airfoil is used with C_L and C_D lookup table for force and moment calculations, the BEMT results did not match accurately with the experimental results.

2.2.2 Forward Flight Performance

Both the lifting force and propulsive force has to be generated during forward flight. Hence the rotor disk has to be tilted forward at an angle of attack to the oncoming flow. Axisymmetric property of the rotor is lost during these conditions and rotors will start flapping. Due to the complex nature of the rotor flow in forward flight, a comprehensive analysis of rotor is required to calculate accurate power. In this thesis, a simple momentum theory is used to calculate the power required by the RWUAV during forward flight. In this theory, the power required can be separated into three components: induced power P_i, profile power P_p and parasitic power P_0.

Profile power is given as,

$$P_0 = \frac{\sigma C_{d_0}}{8}\left(1 + 4.3\mu^2\right)\rho A V_{tip}^3 \tag{2.27}$$

Parasitic power results from viscous shear effects and flow separation on the airframe, rotor hub and so on. Parasitic power is calculated using the equivalent flat plate approach.

$$P_p = \frac{1}{2}\rho V_{tip}^3 f \tag{2.28}$$

Equivalent flat plate area calculated from [26] is given by,

$$f = 0.00217 \times W_{gross}^{0.8357} \tag{2.29}$$

Induced power is given as,

$$P_i = \frac{1}{B} T v_i \tag{2.30}$$

where B is the tip loss factor and T is the thrust required. Tip loss factor for a rotor can be assumed to be 1.15 as given in [20].

2.3 Weight Estimation

The previous section established the mathematical background for calculating RWUAV power during hover and forward flight. In this section, weight estimation formulas are presented for systematically and iteratively determining the gross weight for a given set of design parameters. Performance parameters like payload weight, flight altitude, endurance are specified based on mission requirements given in section 1.1. Weight estimation is mostly based on previous experience and good judgment about existing and future engineering trends. The weight estimates for each component are derived from historical weight data subjected to a mathematical process known as multiple linear regression[25]. This results in equations which are the function of every parameter that affects the component weights. While there are many weight estimation equations available concerning the full-size helicopter preliminary design, there is not much within small size helicopter design, especially in class 0[18]. There are not many openly available class 0 vehicles component weight data and using CAD software will increase the designing time, hence many full-size helicopter weight estimates are studied and compared. With good judgment, the following equations are considered suitable for sizing of a RWUAV.

Main rotor group consists of the rotor blade, hub, and hinge assembly. Equations 2.31 and 2.32 from Naval Postgraduate School[16] is used for the weight estimation of main rotor blade, M_{mrb} and hub hinge assembly, M_{hh} respectively.

$$W_{blades} = 0.06 \times W_{empty} \times R_{mr}^{0.4} \times \sigma_{mr}^{0.4} \tag{2.31}$$

$$W_{hh} = 0.0135 \times W_{empty} \times R_{mr}^{0.42} \tag{2.32}$$

Where R_{mr} is main rotor radius, M_{empty} is empty mass, and σ_{mr} is main rotor solidity.

Tail rotor group weight is estimated using RTL formulas[24]. It gives a good approximation

for class 0 vehicles.

$$W_{tr} = 1.3778 \times (3.28 \times R_{tr})^{3.2808} \times \left(\frac{P_{mr} \times R_{mr}}{Vtip_{mr}}\right)^{0.8951} \times 0.4535 \tag{2.33}$$

Where R_{mr} is main rotor radius, R_{tr} is tail rotor radius, P_{mr} is main rotor power, and $V_{tip_{mr}}$ is main rotor tip speed.

Similar to the tail rotor group, RTL formula is used to estimate structure weight in this design. The structure includes fuselage, horizontal tail, and vertical tail. Fuselage weight is given by,

$$W_{fuse} = 4.59 \times (0.022W_{gr})^{0.5719} \times n_{ult}^{0.2238} \times (3.28L)^{0.5558} \times (10.76S_f)^{0.1534} \times I_{ramp}^{0.5242} \tag{2.34}$$

where length of the fuselage, L_f is calculated using,

$$L_f = 0.824 \times (2 \times R_{mr})^{1.056} \tag{2.35}$$

The area and aspect ratio of horizontal and vertical stabilizers are selected based on existing helicopter data. Their weights can be calculated from equations 2.36 and 2.37.

$$W_{ht} = 0.325 \times (10.76S_{ht})^{1.881} \times AR_{ht}^{0.3172} \tag{2.36}$$

Where S_{ht} is an area of the horizontal stabilizer and AR_{ht} is the aspect ratio of the horizontal stabilizer

$$W_{vt} = 0.471 \times (10.76S_{vt})^{0.9441} \times AR_{vt}^{0.5332} \times n_{gtr}^{0.7058} \tag{2.37}$$

Where S_{vt} is area of vertical stabilizer, AR_{ht} is aspect ratio of horizontal stabilizer, and n_{gtr} is the number of tail rotor gear boxes

Landing gear weight is given by,

$$W_{lg} = 0.015 \times W_{gross} \tag{2.38}$$

Control and electrical weights estimates taken from [20] is given by,

$$W_{control} = 0.06 \times W_{empty} \tag{2.39}$$

$$W_{elec} = 0.06 \times W_{empty} \tag{2.40}$$

Where, W_{empty} is the empty weight of the RWUAV.

Drive system weight estimates are taken from Boeing Vertol formulas[20]. In this approach, the overall drive-system weight of single-rotor configurations is predicted by estimating the weights of the main-rotor and tail-rotor drive systems separately. Equation 2.41 and 2.42 gives the weight of the main rotor drive system.

$$W_{trans} = 250 \times a_{mr} \times \left[\left(\frac{HP_{mr}}{RPM_{mr}}\right) \times Z_{mr}^{0.25} \times K_t\right]^{0.67} \times 0.4535 \tag{2.41}$$

$$W_{trans} = 300 \times a_{tr} \times \left[1.1 \times \left(\frac{HP_{tr}}{RPM_{tr}}\right)\right]^{0.67} \times 0.4535 \tag{2.42}$$

Where, a_{mr} and a_{tr} are adjustment factors, Z_{mr} is number of stages in main rotor drive and k_t is configuration factor. $k_t = 1$ for single rotor configuration and $k_t = 2$ for tandem rotor configuration.

Maximum tail rotor drive system horsepower is given by,

$$HP_{tr} = 0.1 \times HP_{mr} \tag{2.43}$$

Where, HP_{mr} is the maximum main rotor drive system horsepower.

Since the engine for the current design is chosen as mentioned in 2.1. Weight of the propulsion unit is 47kg and kept constant through out the design process.

Fuel weight is calculated from the performance requirements of RWUAV and Fuel flow rate (ffr) of the considered engine. The fuel flow rate of the engine at different altitude and power settings are calculated based on the performance test results from Figure 2.6. The average slope of the fuel flow versus horsepower can be found using values of fuel flow

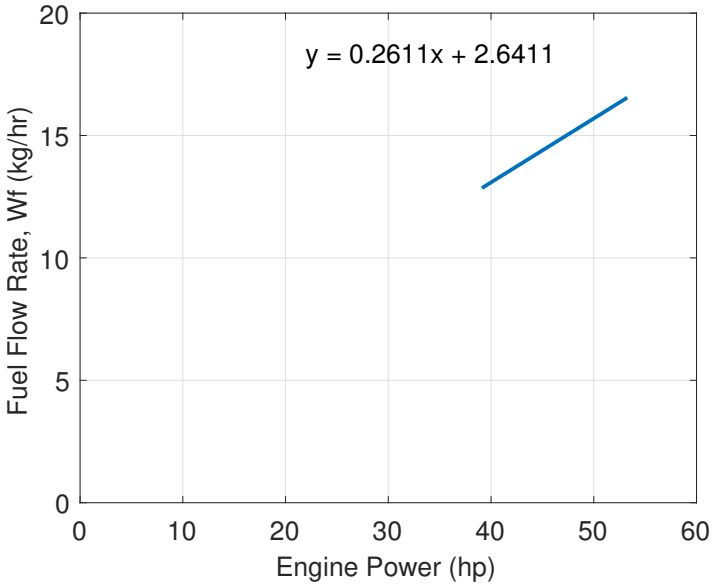

FIGURE 2.6: Performance test results [22] - fuel flow rate vs engine power

rate at the high, normal, and cruise power settings as given in [22]. The intercept of the fuel flow versus horsepower line with the ordinate axis is the Zero Horsepower Intercept (ZHI). At standard sea level, the average slope and ZHI is given as,

$$\beta_{avg} = 0.2611 \tag{2.44}$$

$$\alpha_{avg} = 2.460 kg/h \tag{2.45}$$

ZHI at different altitudes can be determined using equation 2.46. At standard sea level conditions, both temperature ratio θ and pressure ratio δ are equal 1. Hence, α_{avg} is the ZHI.

$$ZHI = \alpha_{avg} \times \delta \times \sqrt{\theta} \tag{2.46}$$

Zero horsepower increment is the power required by the engine when no load is taken from the engine. For maximum endurance flight, the power required from 2.2 should be added with the zero horsepower increment to find the total power to be generated by the engine. The zero horsepower increment is sometimes called as phantom power (P_{hp}). Assuming the slope of the fuel flow vs horsepower line is constant for different altitudes,

Zero horsepower increment can be determined by the Equation 2.47.

$$P_{hp} = \frac{\left[\alpha_{avg} \times \sqrt{\theta} \times \delta\right]}{\beta_{avg}} \tag{2.47}$$

Zero horsepower increment is then added with the power calculation from section 2.2, and fuel flow rate for that forward flight condition can be extrapolated from Figure 2.6. Fuel weight is then calculated using equation 2.48.

$$W_{fuel} = (t_{TO} \times ffr_{NRP}) + (t_{endu} \times ffr_{endu}) + \left(\frac{range \times ffr_{range}}{V_{range}}\right) \tag{2.48}$$

Where t_{TO} is the time for takeoff and landing, t_{endu} is reserve time for cruise at maximum endurance velocity, ffr_{NRP} is the fuel flow rate of the engine at the normal rated power, ffr_{endu} is the fuel flow rate during maximum endurance condition, ffr_{range} and V_{range} is the fuel flow rate and velocity during maximum range condition.

Some systems are not explicitly mentioned in the above-given weight estimates. They include fuel system, avionics, instruments, and anti-icing system. Weight of these systems can be estimated by,

$$W_{fixed} = 0.22 \times W_{gross} \tag{2.49}$$

Where W_{gross} is the gross takeoff weight of the RWUAV.

Weight coefficients used in the above-given weight estimates are given in Table 2.1.

TABLE 2.1: Parameters used in weight estimation formulas

Parameters	**Value**
n_{ult}	2
S_f	0.094 m^2
S_{ht}	0.688 m^2
AR_{ht}	2.5
S_{vt}	1.63 m^2
AR_{vt}	4
Z_{mr}	1
a_{mr}	1
a_{tr}	0.9

2.4 Design Trade Study

For any given payload and performance requirements, several designs can satisfy the constraints. The parametric analysis allows studying the influence of critical design parameters on the sizing of RWUAV. The weight estimation equations, power calculation functions are integrated into a tool that is used for design trade study based on gross weight and hover performance. A flowchart depicting the sizing algorithm and the process is shown in figure 2.7. The required inputs are number of blades, main rotor radius, aspect ratio, tip speed, payload, range, and an initial guess for the GTOW. These design parameters are constrained based on the minimum size required to satisfy the performance requirements and maximum limits of those parameters from statistics[18]. Table 2.2 shows the minimum and maximum limits of the design parameters chosen.

TABLE 2.2: Design parameter set for fuel powered RWUAV

Parameters	**Range**
Number of blades, N_b	2
Radius, R_{mr}	1.8 - 2.4 m
Aspect Ratio, AR_{mr}	6 - 13
Tip velocity, $V_{tip_{mr}}$	153 - 183 m/s

It is observed that a higher number of blades are preferred when the vehicle is heavier and when high power is available at mission altitude. This is because a higher number of blades can generate more thrust for the same RPM, but it also requires more power since it has to overcome the profile drag and power loss due to rotor-rotor interactions. Comparing with many blades system, two blades system is easy to maintain. Hence for small and low weight helicopters, the optimum design will be to have two number of blades. Twist angle is not considered as the primary design parameter in this process since it can be optimized for minimum power after the preliminary sizing of the RWUAV. The initial GTOW is assumed to be thrice the desired payload weight.

Once the primary design parameter set is chosen, tail rotor parameters are sized[26]. The radius of the tail rotor is considered as one-fifth of the main rotor radius, and the tip speed

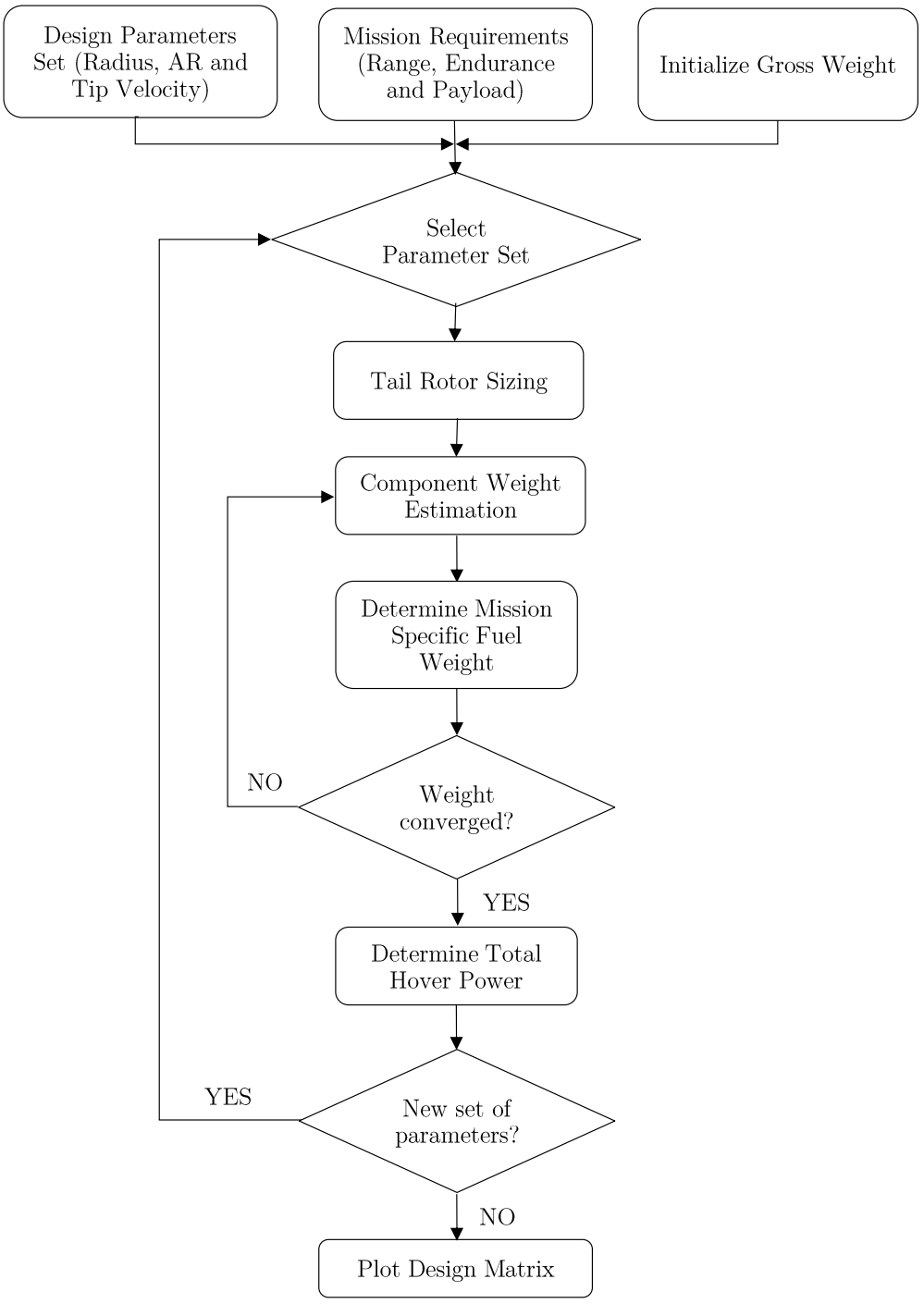

FIGURE 2.7: Design process of a fuel powered RWUAV.

of the tail rotor is considered same as the main rotor tip speed, which makes the rotational velocity of the main rotor five times the main rotor rotational velocity. The tail rotor is sized larger than in [26] because the larger radius is required to counter the same torque at the considered mission altitude than at sea level. The aspect ratio for the tail rotor is assumed to be 6. The distance from the center of the main rotor shaft to the center of the tail rotor shaft, L can be approximated as,

$$L = R_{mr} + R_{tr} + 0.3 \tag{2.50}$$

After tail rotor parameters are determined, RWUAV component weights and fuel weight are estimated based on the weight formulas and power calculation during forward flight given in Section 2.3 and 2.2. Once all the subcomponent weights have been calculated, they are summed into a new GTOW. New GTOW is then compared with initial assumed gross weight. If the difference is within the range, then iteration ends, else the assumed weight is replaced by new weight and component weights are calculated again. This sizing loop goes on until the iteration converges. After estimating the weight, total vehicle power is calculated. This RWUAV design is based on the HOGE power at the considered altitude. HOGE power includes main rotor power, tail rotor power, accessories power, engine efficiency, and transmission power loss. Main rotor hover power is calculated using BEMT explained in section 2.2. Tail rotor thrust required to counter the torque generated by the main rotor is calculated from Equation.2.51. As the thrust required to be generated by the tail rotor is known and assuming that there is no interference of main rotor wake on tail rotor, BEMT is again used to find the tail rotor power required during HOGE.

$$T_{tr} = \frac{Q_{mr}}{L} \tag{2.51}$$

Where T_{tr} is the tail rotor thrust and Q_{mr} is the main rotor torque.

For the accessories power and other power losses, 15% of total power is considered. Total

HOGE power can be expressed as in Equation 2.52.

$$P_{HOGE} = P_{mr} + P_{tr} + P_{acc} + P_{losses} \tag{2.52}$$

The above process is carried out for all the design parameter set and results are given below,

Effect of design parameters on GTOW is shown in Figure 2.8. While Figure 2.9 shows the relationship between the total hover power and design parameters. Each surface on both the figures shows the influence of tip velocity, main rotor radius, and an aspect ratio on GTOW and HOGE power of the RWUAV.

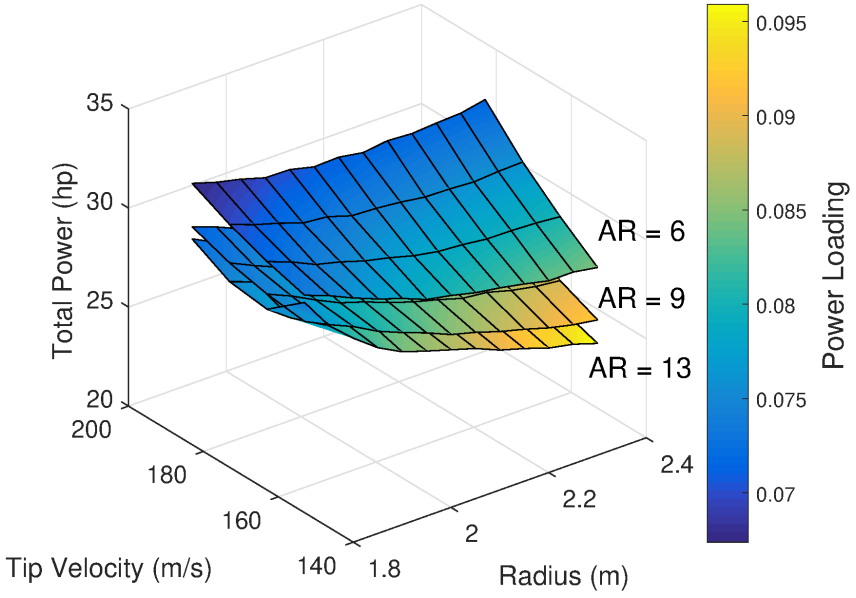

FIGURE 2.8: Variation of hover power with R_{mr}, $V_{tip_{mr}}$ and AR_{mr}

- Each surface plot in Figure 2.8 and 2.7 corresponds to an aspect ratio. The bottom surface corresponds to the aspect ratio of 13 and has the lowest gross weight and hover power while comparing with other two surfaces of aspect ratio 9 and 6. As the aspect ratio decreases, the gross weight and hover power increases for a given radius and tip velocity.

- It is also observed that the GTOW increases while the hover power decreases with increasing main rotor radius. Increasing the main rotor radius increases the disk loading, thereby reducing the induced power but also increases the main rotor blade, hub, and tail rotor group weight.

- For a larger aspect ratio, lower tip velocity requires higher collective pitch angle, thereby increasing the induced power, fuel weight, and gross weight consequently. Whereas for a higher tipspeed, profile power increases hence increasing the gross weight.

- Colour bar in each surface represents the Power Loading of the RWUAV. Power loading (kg/hp) is the measure of hover efficiency of the rotor given by power required to keep the weight of the RWUAV during hover. Increasing the main rotor radius reduces the induced power during hover, thereby increasing the efficiency of the RWUAV.

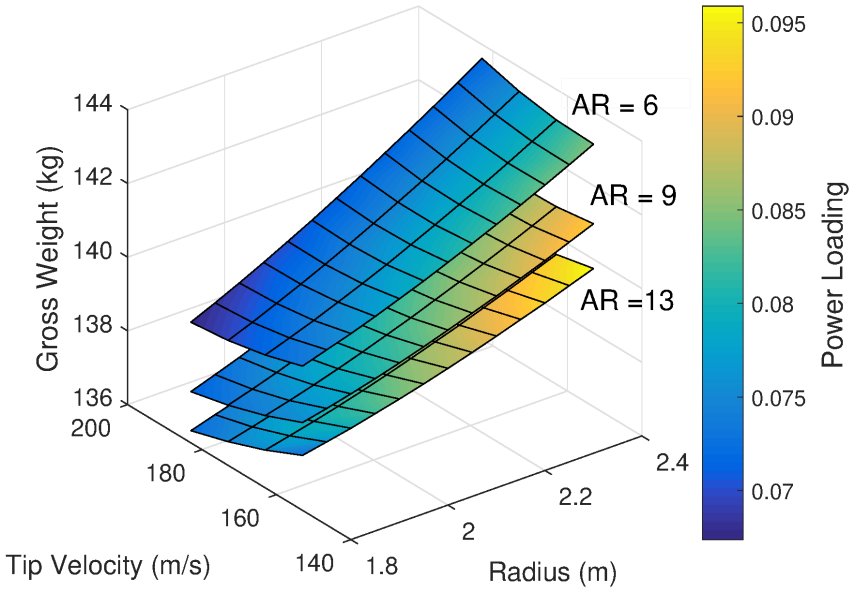

FIGURE 2.9: Variation of gross weight with R_{mr}, $V_{tip_{mr}}$ and AR_{mr}

Figure 2.10 shows the variation of hover power with respect to tip speed for AR = 12 and different main rotor radius. For Radius = 1.8m, lower tip velocity results in a higher

collective pitch angle requirement, which increases the induced power. As the tip velocity increases the power requirement decreases, further increasing the tip velocity increases the profile drag thereby increasing the hover power.

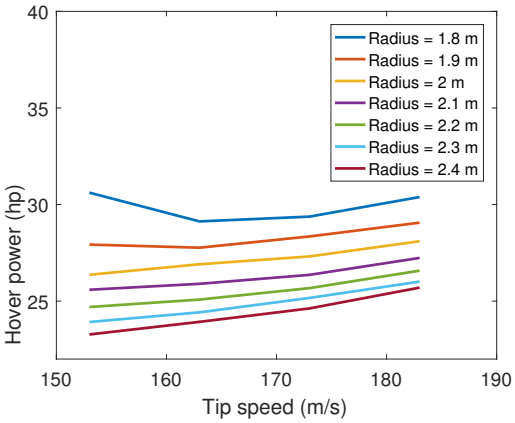

FIGURE 2.10: Variation of hover power with tip speed for AR=12.

2.5 Optimization

Optimization is a process of selecting the best solution out of all the available solutions. In the previous section, it is seen that there is a solution for every parameter set. The selection of design parameters can significantly change the design performance. For the best design, both GTOW and hover power at the mission altitude has to be minimum. From figures 2.8 to 2.9, it can be noted that increasing the main rotor radius increases the GTOW but decreases the hover power. Since both the objectives are conflicting in nature, manual selection of parameters for optimum design is very difficult. Hence a multi-objective optimization using a genetic algorithm is used for selecting optimal design parameters.

2.5.1 Multi Objective Optimization

Multi-objective Optimization is a multi-criteria decision-making method used in problems involving more than one objective functions to be optimized simultaneously. When the objectives are conflicting in nature, there is no single solution that simultaneously optimizes each objective. In these conditions, Pareto optimal solutions exist. A non dominated solution set, where none of the objectives can be minimized without degrading the value of the other objective is called Pareto optimal solutions. All the Pareto optimal solutions can be considered equally good. The goal here is to find a Pareto optimal solution set that defines the best trade-off between Gross weight and Hover power.

Problem statement is given by,

$$min\,(GTOW(x), P_{hover}(x))$$

$$s.t.\ x\ \epsilon\ X,$$

where X is the feasible set of design parameters.

There are four different methods of multi-objective optimization.

- **No preference method**, where preference is not required to identify the optimal solution.
- **Priori method**, where the decision maker is asked to provide preference information that is used to find the best solution.
- **Posteriori method** that presents the Pareto optimal solutions first and then the decision maker is allowed to choose a solution from them.
- **Interative method**, which requires the decision maker's preference input during each iteration. Preference input can vary in each iteration.

In this thesis, a posteriori method with the evolutionary genetic algorithm is used to find the Pareto optimal solutions.

2.5.2 Genetic Algorithm

Genetic algorithm is belonging to an evolutionary algorithm class, as it is based on Charles Darwin's theory of natural evolution and genetics. This algorithm follows the "survival of the fittest" principle by selecting the fittest individuals from a population to produce the best individuals in the next generation.

Below are the steps considered in genetic algorithm,

- **Initial population** - Population is a set of individuals chosen within the search space for GA. Individuals in a population are usually chosen randomly from the search space, which is the entire range of design parameters. Every individual in the population is a possible solution to the given problem.
- **Fitness function** - It determines how fit an individual is and a fitness score is assigned to each.
- **Selection** - Fitter individuals are selected to based on the fitness score, that allows the best individuals to pass on their genes to the next generation. Next step is to generate the population for the next generation using the below methods.
- **Crossover** - After selecting the individuals, crossover between randomly selected bit strings of two individuals will result in two new offsprings that go to the next generation. Since the parent individuals are fitter, this method is most likely to produce the best individuals for the next generation.
- **Mutation** - It randomly changes the individual parents to form offsprings. It is done to maintain diversity within the population.

The process is repeated until a termination condition has been reached. Only the fittest offsprings will survive at the end of the evolution process, that represents the best design solution. The termination condition may be a maximum number of generations or when successive iterations no longer produce better results. "*gamultiobj*" function in MATLAB is used to carry out this multiobjective optimization. All the default parameters are used. The design parameters search space is given in Table 2.2. The number of population selected for each generation is 50.

Figure 2.11 shows the Pareto optimal solutions for the current design problem, and each Pareto optimal design parameter values with their corresponding objective function values are presented in Table 2.3. Any solution from this Pareto optimal set can be considered equally competent. From Figure 2.11, it can be seen that there are solutions that are having low hover power have higher gross weight and also vice-versa.

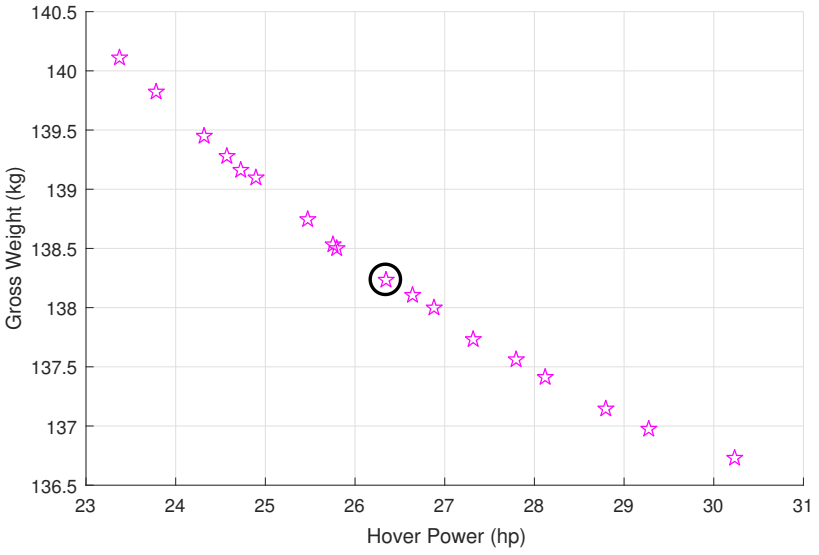

FIGURE 2.11: Pareto optimal solutions for fuel powered RWUAV

Results presented in Table 2.3 shows that all the solutions correspond to an aspect ratio of 13 and for a smaller main rotor radius, higher tip speed is required and vice-versa. A RWUAV that requires lower power to hover is desirable, but the main rotor radius is larger, thus making the vehicle bigger and heavier. While the Wankel engine caps the

TABLE 2.3: List of Pareto optimal solutions for fuel powered RWUAV

S No	**Radius (m)**	**AR**	**Tip speed (m/s)**	**Hover power (hp)**	**GTOW (kg)**
1	1.80	12.96	181.37	30.23	136.72
2	1.81	12.96	175.45	29.27	136.97
3	1.84	12.95	173.6	28.79	137.14
4	1.90	12.94	172.3	28.11	137.41
5	1.98	12.95	171.76	27.31	137.73
6	1.99	12.96	179.3	27.79	137.56
7	**2.04**	**12.92**	**167.95**	**26.64**	**138.10**
8	2.05	12.93	174.10	26.88	137.99
9	2.09	12.95	170.72	26.35	138.23
10	2.12	12.93	166.25	25.79	138.50
11	2.15	12.93	169.67	25.76	138.53
12	2.2	12.94	172.06	25.47	138.53
13	2.23	12.90	163.41	24.90	139.10
14	2.24	12.92	162.63	24.73	139.16
15	2.26	12.94	162.24	24.57	139.28
16	2.27	12.91	157.95	24.32	139.45
17	2.35	12.91	158.11	23.78	139.82
18	2.39	12.89	156.22	23.38	140.11

maximum allowable hover power, extra power should be available during hovering flight at the considered mission altitude. So it is advisable to choose a design, whose hover power requirement is at least 10 percent lesser than the power available at that altitude. The final design is chosen, assuming a tradeoff of 50 percent between both the objectives. The final design selected is highlighted in Table 2.3.

The complete RWUAV design parameter values are given in Table 2.4. Disk loading is the ratio of the gross takeoff weight to the total main rotor disk area. With an Aspect ratio of 12.9, main rotor chord value is 0.158m. Disk loading of the current design is 104 N/m^2. With a main rotor radius of 2.04 m and Tip velocity of 168 m/s, the collective pitch angle required to hover is 9.97 deg. The tail rotor is sized as given in Section 2.4. Tail rotor radius is 0.408 m, and with a tip velocity of 167.9 m/s, collective pitch angle required to counter the torque generated by the main rotor is 8.22 deg.

TABLE 2.4: RWUAV final design parameters

Parameters	**Values**
Main rotor	
No of Blades, N_b	2
Radius, R_{mr}	2.04 m
Chord, c_{mr}	0.158 m
AR	12.92
Tip speed, $V_{tip_{mr}}$	167.9 m/s
Disk Loading, DL	104 N/m^2
Solidity, σ_{mr}	0.049
Collective pitch, $\theta_{coll_{mr}}$	9.97 deg
Tail rotor	
No of Blades, N_b	2
Radius, R_{tr}	0.408 m
Chord, c_{tr}	0.068 m
AR	6
Tip speed, $V_{tip_{tr}}$	167.9 m/s
Solidity, σ_{tr}	0.106
Collective pitch, $\theta_{coll_{tr}}$	8.22 deg

2.6 Performance

Corresponding to the highlighted solution in Table 2.4, induced, profile, and parasitic power along with the total power at 5500 m AMSL is shown in Figure 2.12.

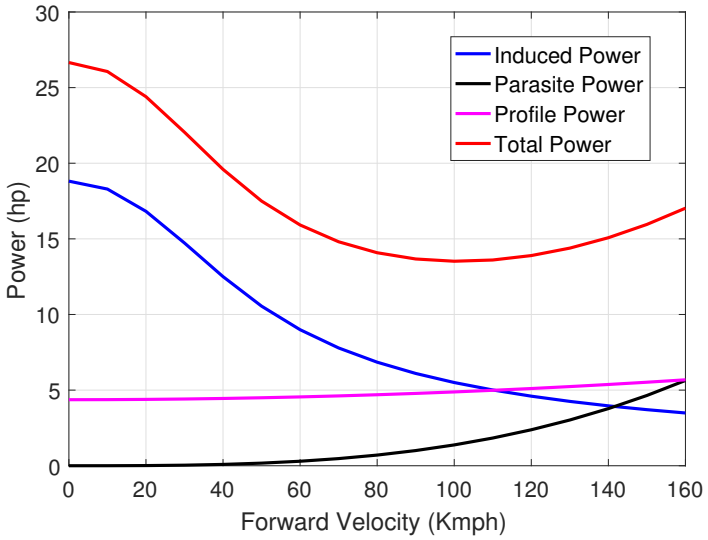

FIGURE 2.12: Forward flight performance of fuel powered RWUAV at 5500 m

As expected, the parasitic power increases with forward velocity while the induced power decreases. Total power includes the accessories power and transmission loss. Cruise velocity is the maximum range condition velocity, and the minimum total power required from Figure 2.12 corresponds to the maximum endurance condition velocity.

All the component weight estimates for the final design are given in Table 2.5. Weight estimation formulas given in Section 2.3 are used to find the weight of the RWUAV components. For a range of 100km and reserve endurance of 15 minutes, fuel weight required is only 6.09kg. For a payload of 20kg, the gross weight of the final design comes to be 138.1 kg. While the structure group weighs 12.6 kg, main rotor and tail rotor group together weigh around 6kg.

TABLE 2.5: RWUAV Vehicle parameters

Parameters	**Values**
Estimated weight	
Main rotor group	5.34 kg
Tail rotor group	0.26 kg
Fuselage	10.8 kg
Empennage	1.797 kg
Propulsion group	47 kg
Landing gear	2.07 kg
Controls	6.7 kg
Electrical	6.7 kg
Transmission	6.6 kg
Fixed	24.62 kg
Empty	111.9 kg
Fuel	6.09 kg
Payload	20 kg
Gross	138.1 kg
Performance characteristics	
Hover power at 5500 m	26.6 hp
Max Range Velocity	140 km/hr
Max Endurance Velocity	100 km/hr
Hover Ceiling	5500 m
Range	100 km
Endurance	1 hr
Power loading	0.083

Performance characteristics of the RWUAV were also given in Table 2.5. Ceiling height of

the RWUAV is assumed to be 5500m even though the power required to hover is less than the power available at that height. Maximum range condition velocity is 140km/hr, and velocity required to fly at maximum endurance condition is 100km/hr.

The final design was chosen with a 10% reserve power while hovering at 5500m AMSL. Reserve power can be used to maneuver the RWUAV in high gust winds, to carry more fuel to extend the range and endurance of the vehicle or deliverable payload can be increased. Figure 2.13 shows the HOGE power at 5500m AMSL when the gross weight is increased. It can be seen that the gross weight of the RWUAV can be 150 kg when the power required to hover is same as the power available from the Wankel engine. There is an extra 12 kg that can be either used as a payload or fuel.

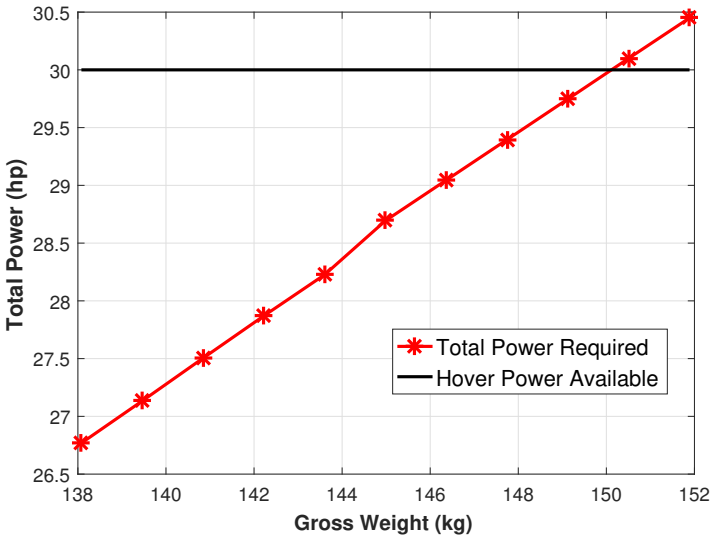

FIGURE 2.13: Extra power available in terms of RWUAV gross weight at 5500 m.

Figure 2.14 shows the range, forward flight, and hover endurance of the RWUAV when the extra weight of 12 kg is added to the fuel weight of the RWUAV. As expected, all the performance values increase with fuel weight. Figure 2.15 shows the range, forward flight, and hover endurance of the RWUAV when the payload is increased from 20 kg to 32 kg. When the gross weight of the RWUAV is 150kg even though the excess power available for hovering at 5500m AMSL will be 0hp, these plots can be used to plan a mission when the requirements are different.

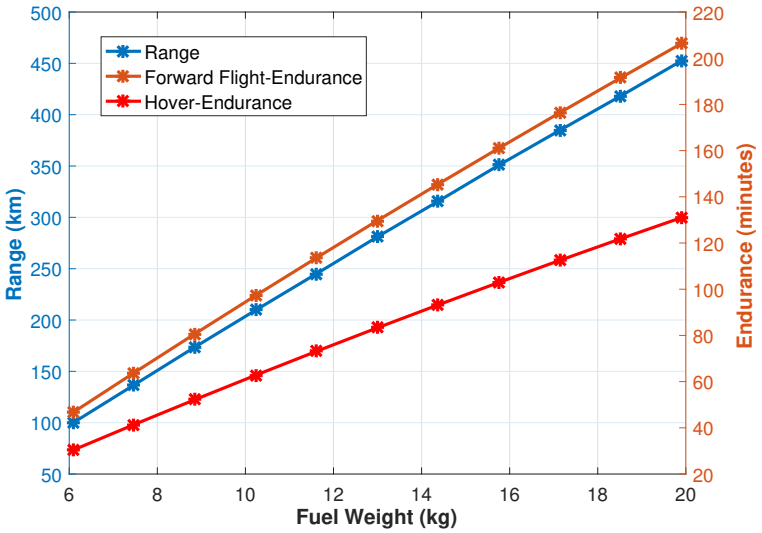

FIGURE 2.14: Performance of the fuel powered RWUAV with increased payload weight at 5500 m.

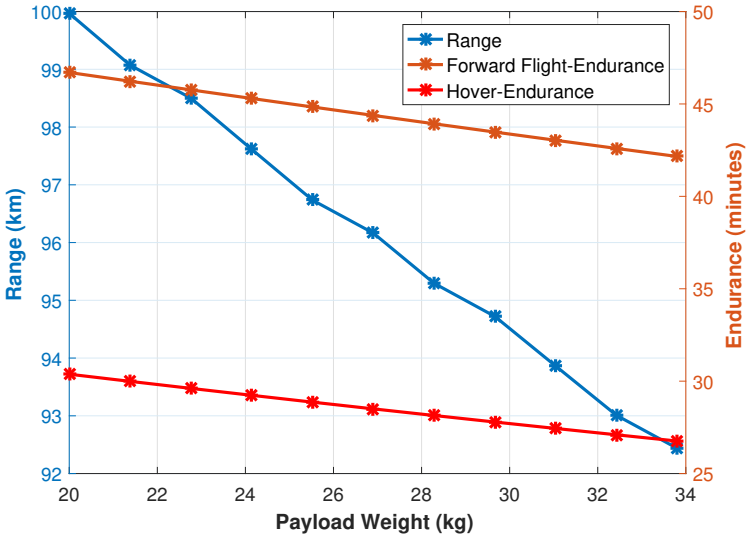

FIGURE 2.15: Performance of the fuel powered RWUAV with increased fuel weight at 5500 m.

The current RWUAV design is compared with a reference autonomous helicopter, Scheibel S-100 Camcopter. Table 2.5 gives a comparison between the design and performance parameters for the current design and Scheibel S100 camcopter helicopter[1]. It can be seen that the estimated empty weight is close to the same weight category RWUAV. Even though the gross weight is less compared to S-100 camcopter, larger main rotor radius is

required to have an efficient hovering flight in higher altitudes.

Table 2.6: RWUAV final design comparison with Camcopter S-100 helicopter

Parameters	**Camcopter**	**RWUAV Design**
Empty weight	110 kg	112 kg
Payload	50 kg	20 kg
Fuel	50 kg	6 kg
Gross weight	200 kg	138 kg
Main rotor Radius	1.7 m	2.04 m
Length	3.11 m	2.75 m
Ceiling	5486 m	5500 m (Hover Ceiling)
Endurance	6 hr	1hr

[1]https://schiebel.net/products/camcopter-s-100/

Chapter 3

Electric Powered Multirotor

This chapter presents the design trade study and preliminary sizing of an electric powered multirotor. Unlike the RWUAV design, the propulsion system is also sized in this process. Momentum theory and Blade Element Momentum Theory that are used to calculate the torque, RPM, and power required during hover and forward flight are explained. Then, component weight estimation formulas that are used to size the multirotor are given. Next, the methodology for the design trade study is illustrated. Finally, the results of the trade study that shows the influence of design parameters on the performance of the design is given.

3.1 Power Calculation

Accurate calculation of power, torque, and revolution-per-minute levels based on rotor geometry and the required thrust helps in accurate sizing of the vehicle. Power with flight time will give the energy capacity of the battery, which determines the battery mass. Power also dictates the current flow in Electronic Speed Controller, which in turn decides the ESC's mass. Power and RPM levels of the motor decide the mass of the motor. Thus power and torque play an essential role in sizing the multirotor components. Same as

RWUAV power calculation, Blade Element Momentum Theory is used to calculate the hover power of the multirotor while momentum theory is used to calculate the forward flight power.

3.1.1 Hover Performance

Blade Element Momentum Theory is the combination of Momentum Theory and Blade Element Theory. In BEMT, inflow characteristics of the rotor are found by equating the incremental thrust coefficients for an annulus of the rotor disk from both the methods. BEMT predicts the loads correctly except at the blade tips. Prandtl's function is used to approximate the tip loss effect on the inflow distribution. This is fully explained in Section 2.2. While a variable pitch rotor is used in RWUAV, a fixed pitch propeller is used in multirotors. Variable pitch rotors have a fixed rotational velocity and thrust is controlled using collective pitch angle. Since a fixed pitch propeller is used in multirotors, RPM of the propeller is used to control the thrust. As in RWUAV power calculation Section 2.2, look up table for CL and CD values of the aerofoil are used to improve the accuracy of the RPM and power calculation.

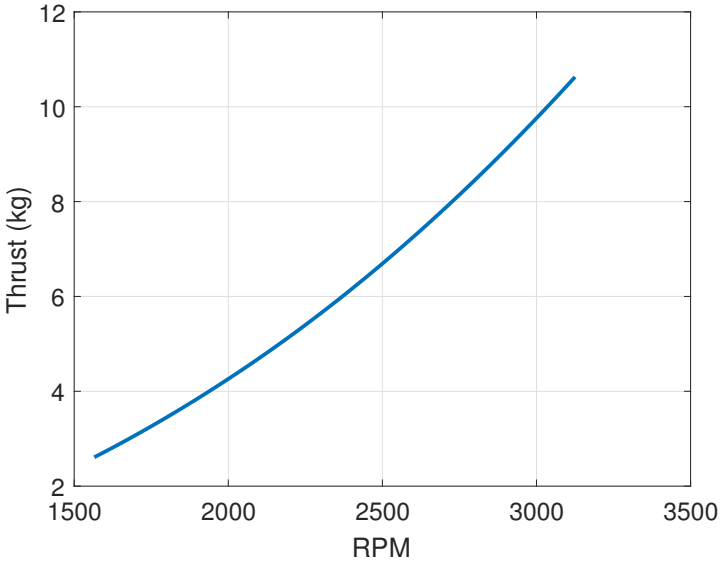

FIGURE 3.1: Thrust vs RPM curve for a fixed pitch propeller.

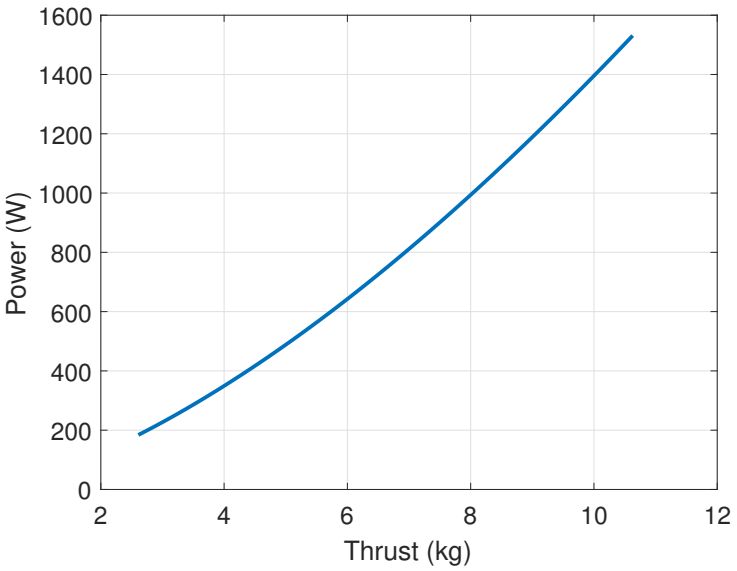

FIGURE 3.2: Thrust vs Power curve for a fixed pitch propeller.

Since RPM of the motor is used to control the thrust of the rotor, constant pitch of 12 deg is assumed for the fixed pitch propeller. The pitch of the propeller can be optimized in the future for both the hover and forward flight performance simultaneously. Performance of the rotor characterized by radius = 0.45 m, chord = 0.075 m and number of blades = 2 at an altitude of 5500m is given in Figures 3.1 and 3.2. Figure 3.1 shows the thrust vs. RPM curve for a propeller of the typical size used in this design process. Figure 3.2 also shows the power required by the rotor to generate the required thrust.

3.1.2 Forward Flight Performance

Multirotor's power required during forward flight can be calculated using the same method described for RWUAV given in Section 2.2. Power required during forward flight can be separated into three components, namely induced power P_i, profile power P_p and parasitic power P_0. Profile power of the multirotor is modeled the same as given in Equation 2.27. As Parasitic power is calculated using equivalent flat plate approach method, flat plate area of 0.2787 m^2 is assumed from NASA wind tunnel test on commercial multirotors [9]. Induced power is calculated from Equation 2.30 given in Section 2.2. In [27], it is advised

to use a tip loss factor of 1.5 for smaller multirotors. Since the rotor radius of the current multirotor design is significantly larger than the one used in [27] and using tip loss factor of full scale helicopter from [20] gives the perfect match with the hover power calculated using BEMT, tip loss factor of 1.15 is used to find the induced power for multirotors during forward flight.

3.2 Weight Estimation

One of the difficult tasks in designing any vehicle is estimating the component weights of the vehicle, which can also be seen from the RWUAV design explained in the previous chapter. Multivariate linear regression technique is used to get the best fit for the component weight from the available data in [27]. While [27] corresponds to micro multirotors, the same method is also used in [7] for parameterization of components of the small to medium sized multirotors. In this thesis, the weight estimation formulas given in [7] is used.

Brushless DC motors are most commonly used electric motors in multirotors for their efficiency in converting electrical energy to mechanical energy. There are two types of BLDC motors, outrunner(OR) and inrunner(IR). As the name suggests, it defines the component of the motor that rotates. When the propeller is directly attached to the motor axle, it is called direct drive design which is used in this multirotor design. In some cases, gearing can be used to run the propeller, which might reduce the motor weight but also makes it mechanically complex. Mass of the motor can be parameterized by the speed constant, K_v measured in RPM/V. Speed constant is defined by how fast the unloaded motor will turn when unit voltage is applied. From [7], it is seen that generally a lower K_v motor with a larger radius and low pitch propeller is efficient than a higher K_v motor with a smaller radius and high pitch propeller. The BLDC motor weight is estimated using the Equation 3.1.

$$W_{motor} = 10^{4.0499} \times K_v^{-0.5329} \tag{3.1}$$

The most important parameter while selecting an ESC is the maximum rated current. The maximum rated current must be sufficiently larger than the motor current so that the ESC does not overheat and fail. The weight of the ESC is estimated using the Equation 3.2.

$$W_{esc} = 0.8421 \times I_{max} \tag{3.2}$$

The efficiency of the propeller is affected by the material from which it is made [7]. The correct combination of propeller radius, chord, number of blades has to be chosen to work efficiently along with the motor. Even though there are many parameters, major parameters that influence the weight of the propeller is the radius and the material from which it is made. In this thesis, propeller made from carbon fiber is used and the weight of the propeller as a function of radius is given in Equation 3.3.

$$W_{prop} = 0.1207 \times (2R)^2 - 0.05555 \times (2R) + 2.455 \tag{3.3}$$

Batteries are of two types, either primary batteries that cannot be recharged or secondary batteries that can be recharged and used again. The secondary batteries are defined by chemical composition like Lithium Ion (LiIon), Lithium Polymer (LiPo), NiCd, NiMH, and LFP. The specific energy density, discharge rate and efficiency of the batteries are determined by their composition mentioned above. Other than composition, battery cell configuration and capacity are also considered for estimating the weight of the battery. Batteries can be stacked in series to increase their voltage or in parallel to increase their capacity. Capacity is measured in mAh and determines the energy stored in the battery. LiPo batteries are the most commonly used in RC aircrafts and multirotor. In [7], LiPo batteries with different cell configuration and capacities are surveyed and multivariate linear progression technique is used to estimate the weight of the battery as a function of cell configuration and capacity as given in Equation 3.4.

$$W_{battery} = \left(0.0263 \times S + 2.0499 \times 10^{-5}\right) \times C \tag{3.4}$$

Weight of the wiring, including all the power lines, is assumed to be 5% of the GTOW and given in Equation 3.5.

$$W_{wiring} = 0.05 \times W_{gross} \tag{3.5}$$

Structural weight of the multirotor is assumed to be 19% of the GTOW in [7] from the survey taken for lightweight and medium weight multi-rotors. A survey of commercially available heavy payload carrying multi-rotors[1]is given in the Figure 3.3 and from the data, the weight of the airframe is assumed to be 15% of the GTOW as given in the Equation 3.6.

$$W_{airframe} = 0.15 \times W_{gross} \tag{3.6}$$

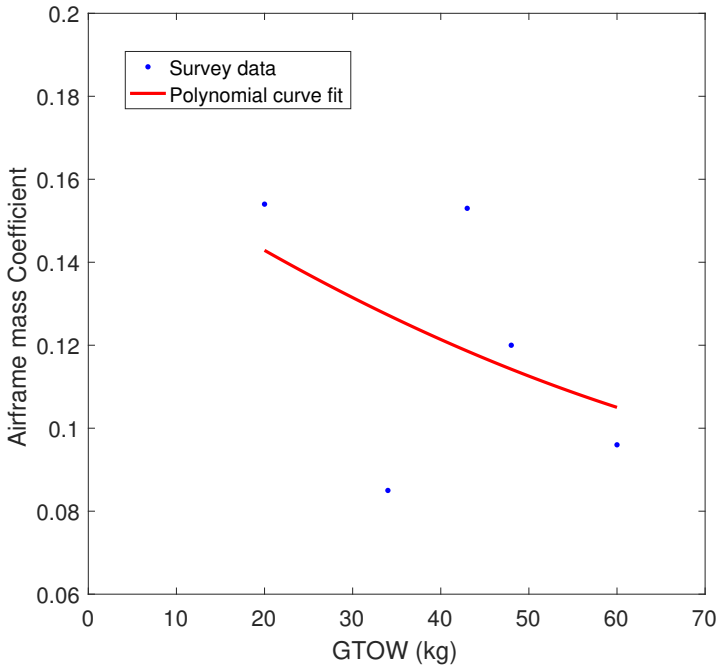

FIGURE 3.3: Survey of available multirotors for airframe mass coefficient

[1]http://vulcanuav.com/aircraft/
[1]https://www.foxtechfpv.com/industrial-drone/heavy-lift-drone.html

3.3 Design Trade Study

Power calculation method and weight estimation equations are integrated into a sizing tool which uses a parametric analysis of design variables based on a mission requirements to come up with an optimal design solution. A high-level flowchart depicting the algorithm is shown in Figure 3.4. It should be noted that the design trade study is based on the hover power of the vehicle at the mission altitude while the study can also be extended based on the forward flight performance. The required inputs are number of rotors, number of blades per each rotor, number of battery cells in series, rotor radius, aspect ratio, payload, range, and an initial guess for the GTOW. These design parameters are constrained based on the minimum size required to satisfy the performance requirements. Table 3.1 shows the minimum and maximum limits of the design parameters chosen.

TABLE 3.1: Design parameter set for electric powered multirotor

Parameters	**Range**
Number of rotors, NOR	8 - 16
Number of blades per each rotor, N_b	2
Number of battery cells in series, S	6 - 12
Radius, R	0.45 - 0.6 m
Aspect Ratio, AR	6 - 12

Performance parameters are given in Section 1.1. Initial gross weight is assumed to be thrice the desired payload weight. In this study, multirotor is sized for a minimum weight and minimum energy conditions. Hover power and RPM is calculated using BEMT assuming the weight of the vehicle is equally shared by all the rotors. Propeller weight is estimated directly from the input design parameters. BLDC motors can operate at different voltage for different power requirements. Low power motors have low working voltage while high power motors have high working voltage. Based on the power requirement of the motor, the Number of cells to be connected in series for the battery is decided.

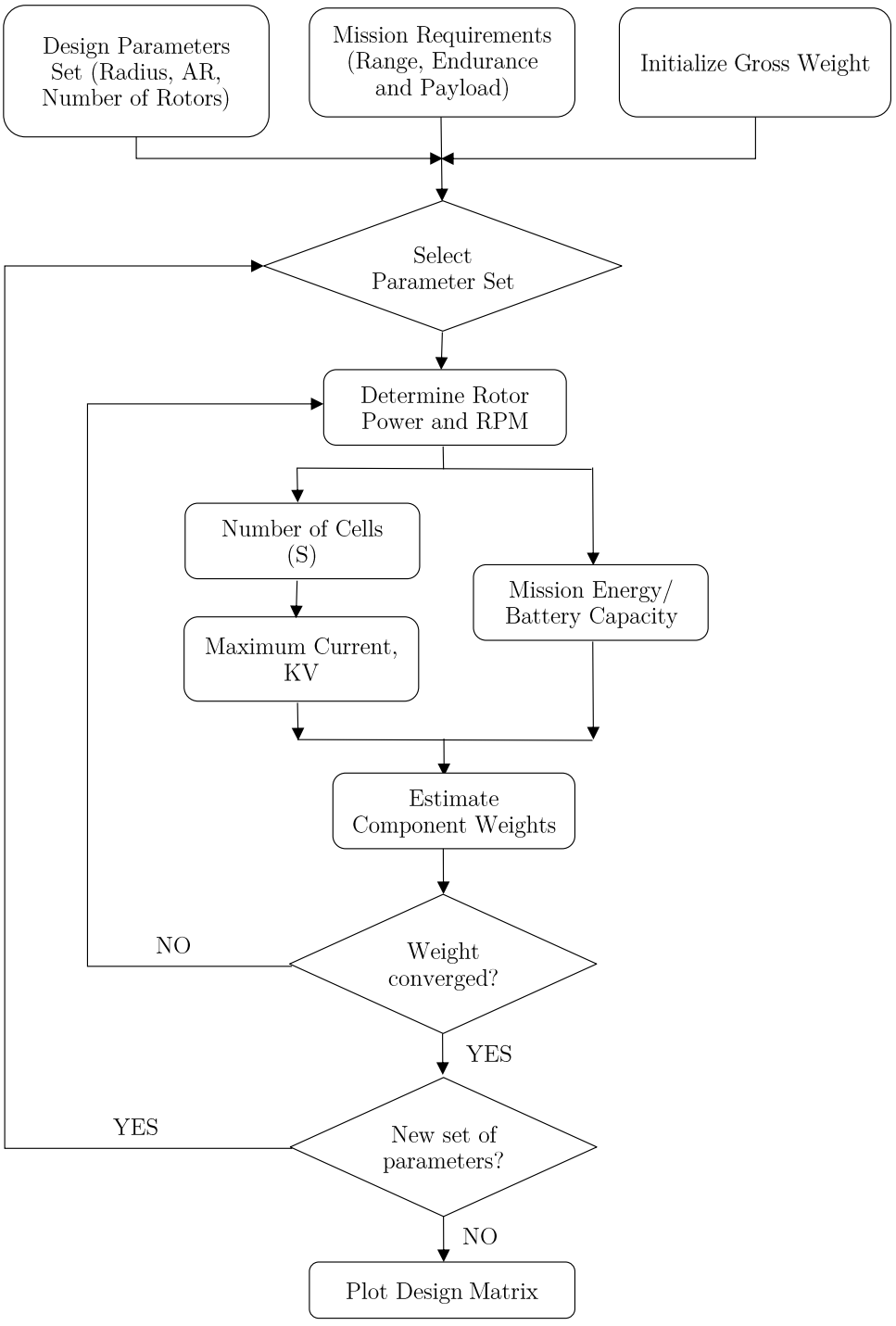

FIGURE 3.4: Design process of a electric powered multirotor.

RPM level found from the BEMT along with voltage of the battery is used to find the speed constant of the motor which determines the weight of the motor. The hover power

divided by the voltage to give the maximum rated current, I_{max} of the motor. I_{max} is then used to size the ESC. Forward flight power is calculated from Section 3.1. Hover power and forward flight power is then multiplied with their respective flight time from mission requirement to find the energy required to be stored by the battery. Dividing the energy by the working voltage gives the capacity of the battery measured in mAh.

Along with the number of battery cells connected in series, capacity of the battery is used to estimate the weight of the battery. Wiring weight and airframe weights are estimated from Equations 3.5 and 3.6. Sum of all the components is used to find the gross weight of the multirotor. Gross weight is then compared with the initial weight assumed. In case the difference is not within the tolerance value, the initial weight is incremented and iteration continues until the weight converges. After the iteration converges for a parameter set, the next set is chosen, and the loop continues until all the possible design parameters are studied.

Since NOR considered in this study is more than 8, all the configurations are assumed to be coaxial. For instance, if NOR is 10 then the multirotor has five arms with two motor-propeller combinations in each arm. BEMT is used to calculate the hover power of the upper rotor while the lower rotor operating in the wake of the upper rotor experiences more induced velocity, which increases the induced power of the lower rotor. BEMT can be modeled to find the power of both the upper and lower rotors since it increases the computation cost and for simplicity, a factor of 1.1 is multiplied with upper rotor hover power to calculate the lower rotor hover power.

In this study, internal resistance and current flow through the motor and ESC are not modeled. Hence an efficiency of 80% is assumed for the motor and ESC combination.

In many batteries, its full capacity cannot be used without causing severe damage to the battery, which is defined by the depth of discharge. Hence the capacity of the battery is multiplied by a factor of 1.15 while sizing the battery.

Exact multirotor components are not chosen using this study, but the parameters (K_v, S, I_{max}, Capacity) of the components are found. Using these parameters, specific drive components can be selected from the database or found from off-the-shelf components.

3.4 Results

In this thesis study, attention is given on the designs that need minimum mission energy at minimum gross weight but still comply with all the mission requirements. Variation of each design parameter given in Table 3.2 is plotted, and an optimal design solution is chosen. This design trade study gives the gross weight, mission energy, other multirotor component parameters for the selected NOR, R, AR, S, and mission requirement. Figure 3.5 shows the results of a variation of NOR and R with gross weight for a multirotor configuration performing the mission given in Section 1.1. Variation of NOR and R on multirotor gross weight is studied for a constant AR = 6 and S = 12.

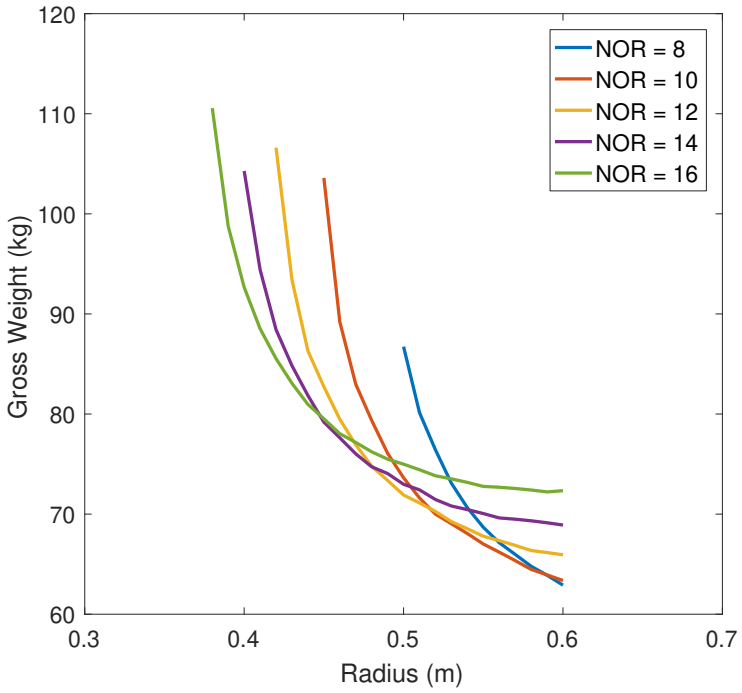

FIGURE 3.5: Influence of NOR and R on gross weight for S=12 and AR=6.

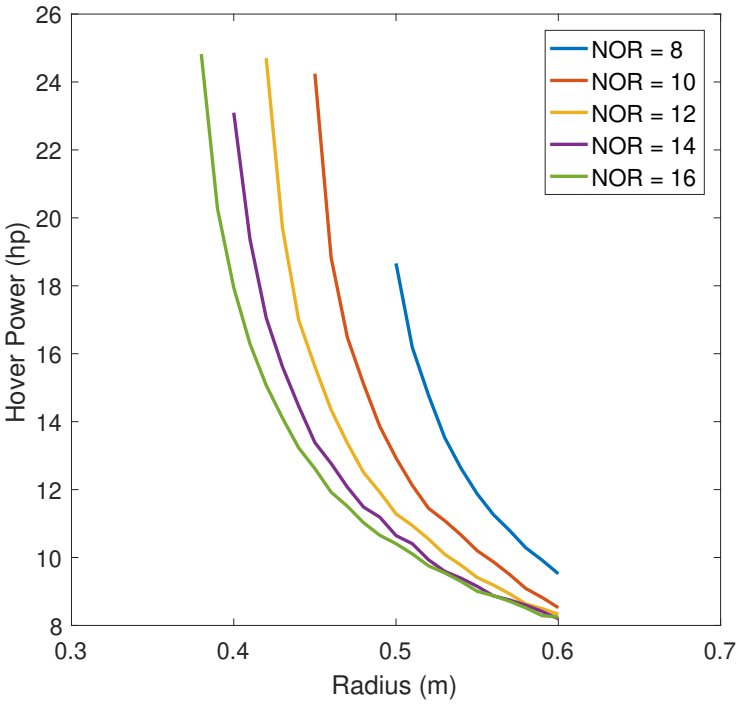

FIGURE 3.6: Influence of NOR and R on HOGE power for S=12 and AR=6.

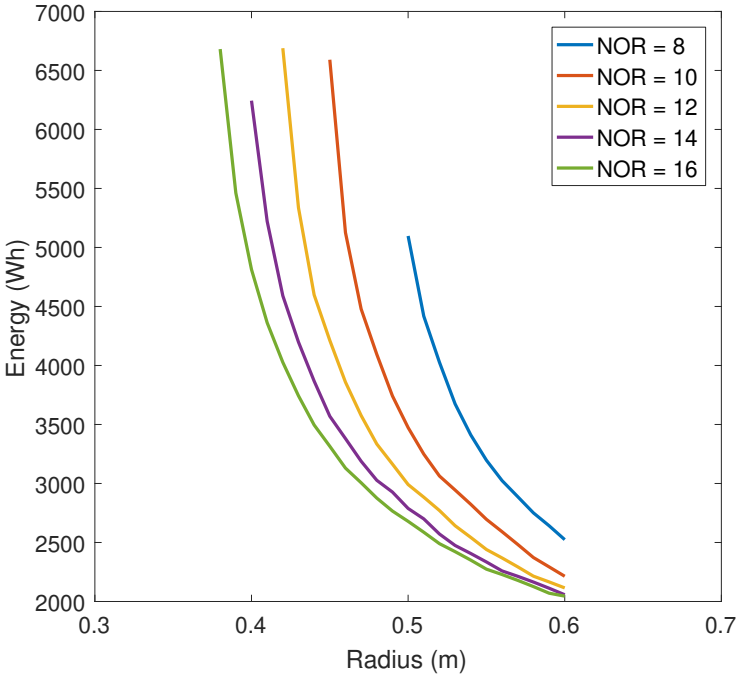

FIGURE 3.7: Influence of NOR and R on mission energy for S=12 and AR=6.

For any NOR, there is a blade radius for which the mission energy and gross weight is significantly large and as the radius is increased both the energy and gross weight reduces.

As expected, for a smaller NOR solutions are possible only with larger radius comparing larger NOR. This plot explains that for a given gross weight, less NOR with larger radius is efficient than a more NOR with a smaller radius.

Figures 3.6 and 3.7 shows the variation of NOR and R with HOGE power and mission energy required by the multirotor, respectively. It shows that the multirotor HOGE power and mission energy declines with an increasing radius for a given NOR and also for increasing NOR for a given R. This trend is noticed from the Figures 3.6 and 3.7 for the chosen range of design parameters, constant AR = 6 and S = 12.

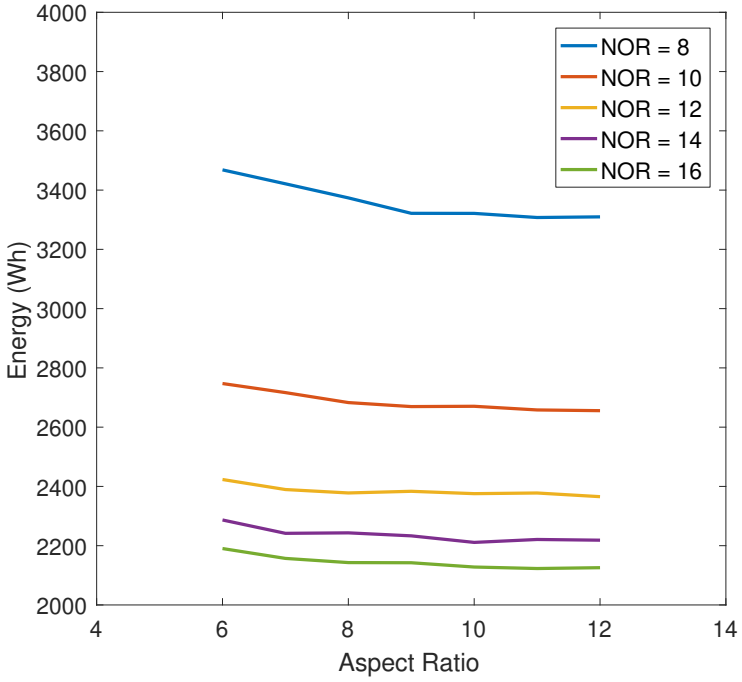

FIGURE 3.8: Influence of NOR and AR on mission energy for S=12 and R=0.5 m.

Effect of aspect ratio for a constant NOR, R and S is given in Figures 3.8, 3.9 and 3.10. Constant blade radius of 0.5 with NOR=12 and S=12 is chosen for the studies. Figures 3.8 and 3.9 shows that the mission energy and HOGE power declines with the increase in the NOR. Further increase in NOR may result in higher mission energy and HOGE power for multirotor.

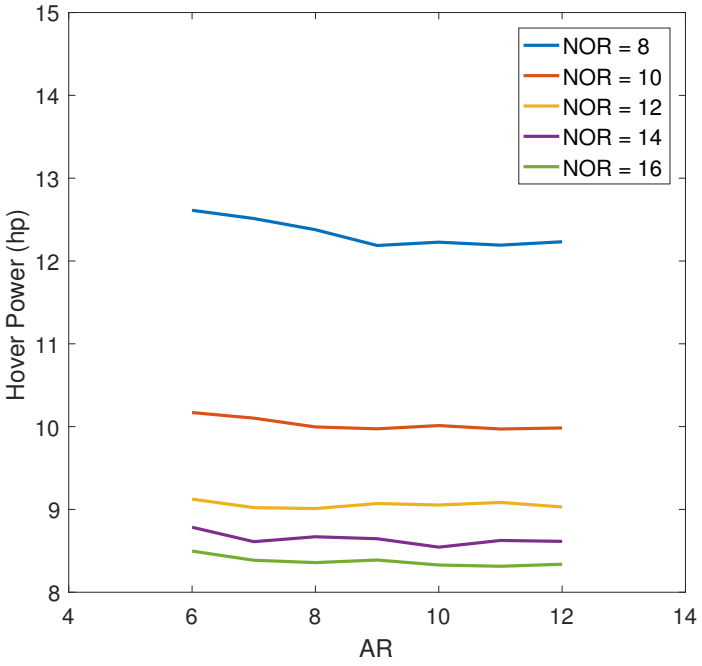

FIGURE 3.9: Influence of NOR and AR on HOGE power for S=12 and R=0.5 m.

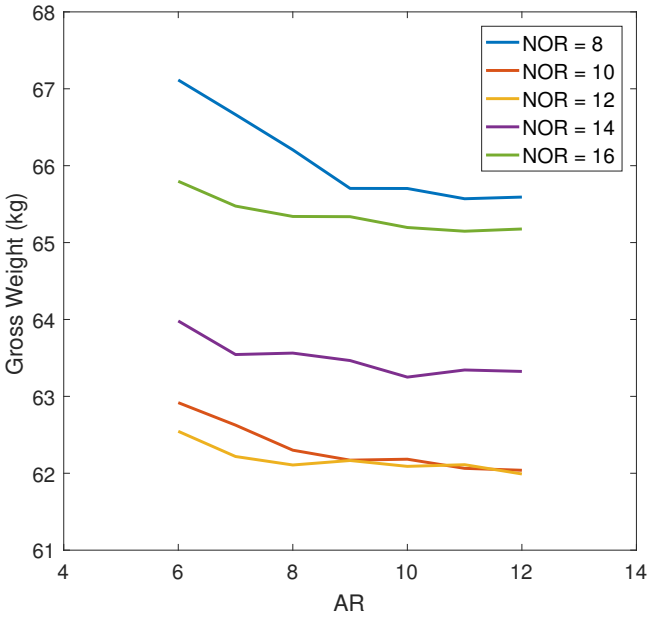

FIGURE 3.10: Influence of NOR and AR on gross weight for S=12 and R=0.5 m.

However, as shown in Figure 3.8, gross weight decreases initially for the increase in NOR,

it starts increasing again when NOR is further increased. It can be seen that NOR=12 gives the minimum gross weight for the mission considered. Even though the AR does not change the mission energy, gross weight, and HOGE power significantly at higher aspect ratios, but it slightly increases for lower aspect ratio.

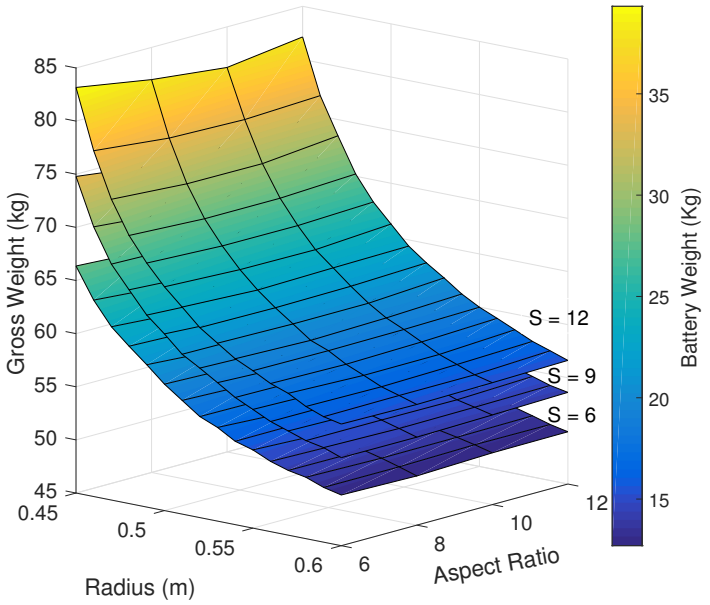

FIGURE 3.11: Influence of R, AR and S on gross weight for a constant NOR = 12.

S is the number of battery cells that are connected serially, it determines the nominal voltage of the battery. Figures 3.11 and 3.12 shows the variation of R and AR on the gross weight and hover power, respectively. Each surface corresponds to one value of S, as given in the figure. While Colour bar in Figure 3.11 shows the battery weight of the multirotor designs, Figure 3.12 shows the power loading of the multirotor during hover at the mission altitude. It can be seen that increasing the working voltage increases the gross weight; this is mainly due to the increase in battery weight because of stacking the cells serially. For any motor that is capable of turning a propeller of radius, more than 0.4 m needs at least an operating voltage of 40V. With LiPo batteries, at least 12 cells are required to be connected serially to achieve this voltage. Even though S=6 gives lower energy and gross weight, S=12 is chosen for the final design for the above mentioned reasons.

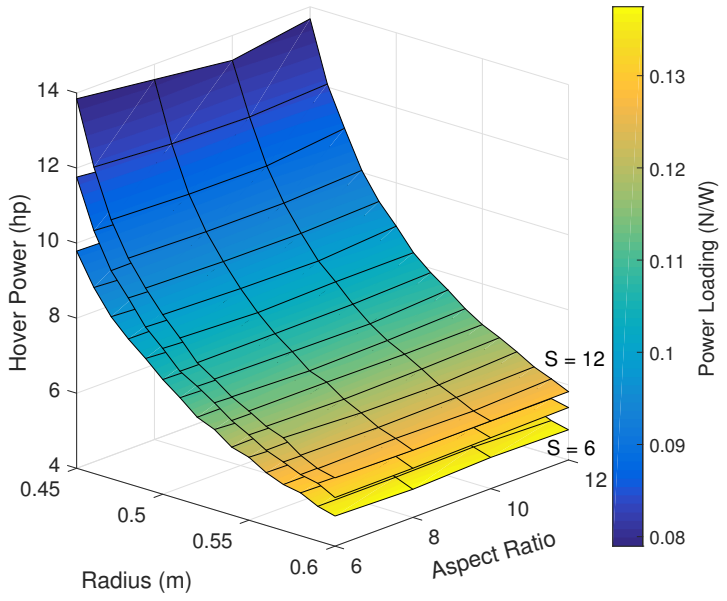

FIGURE 3.12: Influence of R, AR and S on HOGE power for a constant NOR = 12.

The objective of this design process is to achieve a design with minimum weight and minimum mission energy, but minimum blade radius is also preferred, which defines the physical size of the multirotor. Assuming minimum gross weight and minimum radius is the objective, the possible solutions that are selected from Figure 3.5 are given in Table 3.2, and the final design that is selected is highlighted.

TABLE 3.2: List of possible solutions from design trade study for multirotors

S No	NOR	R (m)	AR	S	GTOW (kg)	Energy (Wh)	HOGE Power (hp)
1	10	0.52	6	12	70	3063	11.45
2	**12**	**0.5**	**6**	**12**	**71.91**	**2991**	**11.28**
3	14	0.48	6	12	74.73	3027	11.48

The complete multirotor design parameter values are given in Table 3.3. Number of rotors are 12 while there are two blades per each rotor. Motor with 0.5 m blade radius combination has to run at an RPM of 1903 to generate the required thrust of 6 kg. The solidity of the rotor is 0.106. Speed constant of the motor selected is around 72 while the maximum current the motor derives while hovering at mission altitude is 16 A. The required capacity of the battery is 79Ah with a 12S configuration.

TABLE 3.3: Multirotor final design parameters

Parameters	**Values**
Rotor	
No of rotors, NOR	12
Configuration	Coaxial
No of blades, N_b	2
Radius, R	0.5 m
Chord, c	0.083 m
AR	6
Solidity, σ	0.106
RPM	1903
Propulsion	
No of cells in series, S	12
Speed constant, K_v	72
Max Current, I_{max}	16 A
Capacity, C	79623 mAh

All the component weight estimates for the final design are given in Table 3.4. Weight of the components given in Table 3.4 includes the weight of individual component multiplied by NOR except for the airframe and battery weight.

TABLE 3.4: Multirotor weight estimates and performance characteristics

Parameters	**Values**
Estimated weight	
Rotor	2.03 kg
Motor	13.73 kg
ESC	0.16 kg
Airframe	10.7 kg
Empty	26.7 kg
Battery	25.2 kg
Payload	20 kg
Gross	71.9 kg
Performance characteristics	
Max Endurance Velocity	70 km/hr
Hover Ceiling	5500 m
Hover Power at 5500 m	11.28 hp
Mission Energy	2991 Wh
Endurance	0.5 hr

For a hover endurance of 6 minutes and forward flight endurance of 24 minutes, battery weight required is 25.2 kg. For a payload of 20 kg, the gross weight of the final design comes to be 71.9 kg. While the structure of the multirotor weighs 10.7 kg, rotor and

motor group together weigh around 15.9 kg. The final multirotor design parameters are compared with an already existing multirotor of the same size, GAIA 190MP. Table 3.5 gives a comparison between the design and performance parameters for the current design and GAIA 190MP multirotor.

TABLE 3.5: Multirotor final design comparison with GAIA 190MP multirotor

Parameters	**Multirotor Design**	**GAIA 190MP**
NOR	12	6
Radius	0.5 m	0.43 m
Battery weight	25 kg	16 kg
Payload weight	20 kg	25 kg
Empty weight	26.7 kg	20 kg
Gross weight	71.9 kg	61 kg
Endurance	30 min	15 min
	Hover - 6 min	Hover IGE
	Forward flight - 24 min	

Chapter 4

Electric Powered Conventional Helicopter

This chapter presents the design trade study and preliminary sizing of an electric powered RWUAV. Like Wankel engine used for fuel powered RWUAV design, an electric motor is selected with the same power for this vehicle design. Power calculation methods and weight estimation formulas are the same as the previous two designs. Battery technology is explored, and the selection of a suitable battery for this vehicle design is explained. Design trade study process that allows studying the influence of design parameters on the vehicle design is explained, and finally, the results are presented.

4.1 Engine Selection

In Chapter 1 for fuel powered RWUAV design, Wankel engine with continuous available power of 30 hp at mission altitude is used. For the same continuous power available condition, a survey of electric motors is done. The data for available electric motors[1]is given in Figure 4.1. It shows the gross weight of the electric motor in terms of its continuous available power. The weight of the electric motor is around 8 kg when continuous power

available is 25kW or 30hp. Hence the weight of the electric motor is assumed constant as 8kg, and the weight of the ESC[2]corresponding to this motor is 1.5 kg. The operating voltage of this category electric motor is 120 V.

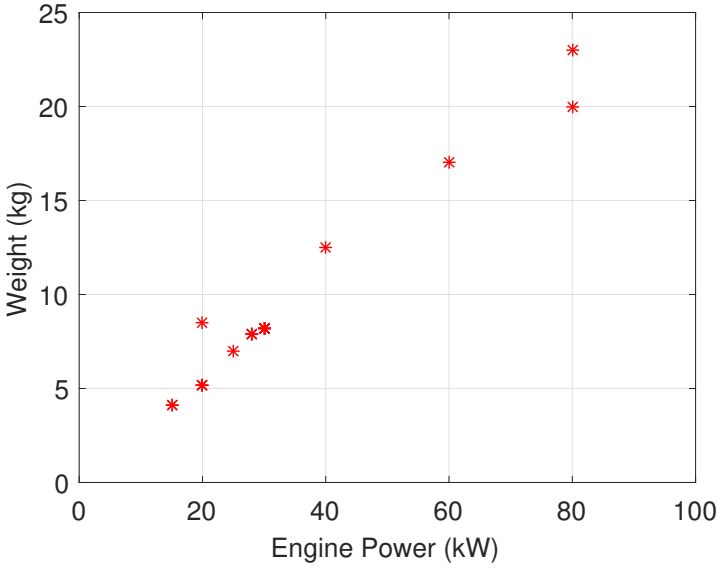

FIGURE 4.1: BLDC electric motor survey.

4.2 Batteries

The battery is an energy source that can deliver power to a device. There are two major types of batteries, non-rechargeable or primary batteries and rechargeable or secondary batteries. Primary batteries are single use; once they are fully discharged, they should be recycled while the secondary batteries can be recharged and reused based on their lifetime. Most commonly used primary battery is Lithium primary battery and mercury battery in watches, cameras, etc.. Secondary batteries are commonly used in electronics like cell phones, laptop, power tools, electric vehicles, etc.

Depending on their chemical compound used, Lithium-ion batteries can produce voltage from 1.5 V to 3.7 V. The batteries must be chosen such that there is sufficient voltage

[1]http://www.rotexelectric.eu/products/bldc-motors/
[2]https://downloads.mgm-compro.com/hbc-manual-lv-mv-50063-280120-270416-a-eng.pdf

required to power the components. The operating voltage of the battery is increased by connecting several battery cells in series, and the capacity of the battery is increased by connecting battery cells in parallel. The capacity of the battery is denoted in Ah. A 100Ah battery can provide 100A of current continuously for 1 hour. Usually, batteries are not discharged completely and discharge rate "C-rating" indicates the discharging capability of the battery.

Based on their chemical compound used, these batteries have different specific energy density. Specific energy density is the amount of energy stored per unit mass of the battery. It defines how much energy can be stored in a battery for a given mass. Nickel-Cadmium (NiCd) and Nickel Metal Hydride are used in RC vehicles earlier, whereas now Lithium polymer (LiPo) batteries have replaced them. LiPo batteries can have specific energy density up to 250 Wh/kg.

Lithium Ion (Li-ion) batteries which have higher specific energy than LiPo batteries are used in Electric vehicles like Tesla. Li-ion batteries have lower maximum discharge rates. Other batteries are Lithium iron phosphate (LiFe) that have a specific energy density of 100Wh/kg, even though they are heavier than Li-ion batteries they are very stable under discharge and damage. For solar aircraft programs, Li-ion batteries are used with an energy density of 220 Wh/kg. The Zephyr 7 uses Lithium-sulfur (Li-S) batteries, with an energy density of 350 Wh/kg, produced by Sion Power Corporation. Lithium Ions batteries are most commonly used in many electric aircraft programs.

Solid state batteries use solid electrodes and solid electrolytes, unlike liquid electrolytes found in lithium-ion batteries. Even though the specific energy density of solid-state batteries are 2.5 times higher than Li-ion batteries, they are expensive to make and have not been used in any successful electric aircraft programs yet.

The Lithium-ion battery is used in this design, and the specific energy density of 250Wh/kg is considered. Considering a 3.6 V Li-ion battery, 36 battery cells are stacked serially to achieve a nominal voltage of 120 V as given in Section 4.1.

4.3 Power Calculation

Both the design process explained in Chapters 2 and 3 uses Momentum theory and Blade Element Momentum Theory for power calculation during forward flight and hover, respectively. A conventional helicopter is controlled using main rotor collective pitch, cyclic pitch and tail rotor collective pitch angles. While variable pitch rotor is used for both the main rotor and tail rotor, a fixed pitch rotor which is controlled by RPM is used in multirotor applications. In this electric powered RWUAV design, a variable pitch propeller is used in the main rotor, and a fixed pitch propeller is used in the tail rotor. During hover condition, the collective pitch angle that is required to generate the thrust by the main rotor and the RPM required by the tail rotor to counter the torque generated by the main rotor are found using BEMT. It is explained completely in Sections 2.2 and 3.1.

As explained in Section 2.2, due to the complex nature of the rotor flow in forward flight, a simple momentum theory is used during the preliminary design stage. It reduces the computational cost and time. This design uses the momentum theory, as explained in Section 2.2 for calculating the forward flight power.

4.4 Weight Estimation

Unlike a conventional helicopter, electric powered RWUAV runs on two separate electric motors, one on the main rotor and another on the tail rotor. By using two different electric motors, weight is reduced considerably by neglecting transmission drive in the design and efficiency is also improved. Even though the main rotor is turned by an electric motor, swash plate, and hub assembly is used to control the rotor using collective and cyclic inputs. While the tail rotor is controlled using the RPM of the motor.

Since the structure of this electric powered RWUAV is same as the fuel powered RWUAV designed in the Chapter 2, Weight estimation of main rotor group, fuselage, horizontal

tail, vertical tail, controls, electrical, landing gear, and other fixed components are done using the formulas given in Section 2.3.

Weight of the electric motor and its corresponding ESC weight is given in Section 4.1. It is considered to be constant throughout the design process.

Tail rotor group of this electric powered RWUAV includes tail rotor, electric motor, and an ESC. Electric motor and rotor combination is sized based on the thrust required by the tail rotor to counter the torque generated by the main rotor. Weight estimation equation given in Section 3.2 is used to calculate the tail rotor group weight since the electric motor and rotor required comes within the range of data used in Section 3.2.

The energy required to be stored by the battery is given by the mission requirement and the power required by the RWUAV for hovering and forward flight at mission altitude. Considering a specific energy density of 250 Wh/kg for Li-ion batteries, the weight of the battery is calculated using the Equation 4.1.

$$W_{battery} = \frac{Mission\ Energy\ (Wh)}{Specific\ energy\ density\ (Wh/kg)} \tag{4.1}$$

4.5 Design Trade Study

Design trade study allows studying the influence of critical design parameters on the sizing of electric powered RWUAV. This allows us to choose a solution from a set of a possible solution that satisfies the mission requirements. The process used for designing a fuel powered RWUAV, and a multirotor is combined to design an electric powered conventional helicopter with tail rotor configuration. The process is outlined in Figure 4.2. The required inputs are number of blades, main rotor radius, aspect ratio, tip speed, payload, range, and an initial guess for the GTOW. The design parameters are constrained based on data parameter values used in Chapter 2. Table 4.1 shows the minimum and maximum limits of the design parameters chosen.

TABLE 4.1: Design parameter set for electric powered RWUAV

Parameters	**Range**
Number of blades, N_b	2
Radius, R_{mr}	1.8 - 2.3 m
Aspect Ratio, AR_{mr}	12 - 16
Tip velocity, $V_{tip_{mr}}$	140 - 180 m/s

Similar to fuel powered RWUAV and as mentioned in Section 2.4, Number of blades in the main rotor is two and the twist angle is not considered as the primary design parameter. The design process starts by choosing a parameter set, and a guess for an initial gross weight. Initial gross weight is guessed based on the literature data or three times the payload weight can be taken. Once the primary design parameter set is chosen, tail rotor parameters are sized[26]. The radius of the tail rotor is considered as one-fifth of the main rotor radius, and the tip speed of the tail rotor is considered same as the main rotor tip speed, which makes the rotational velocity of the main rotor five times the main rotor rotational velocity. The aspect ratio for the tail rotor is assumed to be 6. As mentioned in Section 4.3, BEMT is used to calculate HOGE power. Thrust required to be generated by the tail rotor is calculated by dividing the torque of the main rotor by the distance between the main rotor shaft and tail rotor shaft. Collective pitch angle required of the main rotor and RPM of the tail rotor is calculated separately using BEMT. For the accessories power and other power losses, 15% of total power is considered. Total HOGE power can be expressed as in Equation 4.2.

$$P_{HOGE} = P_{mr} + P_{tr} + P_{acc} + P_{losses} \tag{4.2}$$

After tail rotor parameters and hover power are determined, tail rotor weight is estimated directly from the tail rotor parameters. Operating voltage for tail motor is assumed to be 48 V. From RPM level determined from BEMT and operating voltage, speed constant K_v is calculated, which determines the motor weight. Power required by the tail rotor and operating voltage dictates the maximum current flow in the motor and thus determining

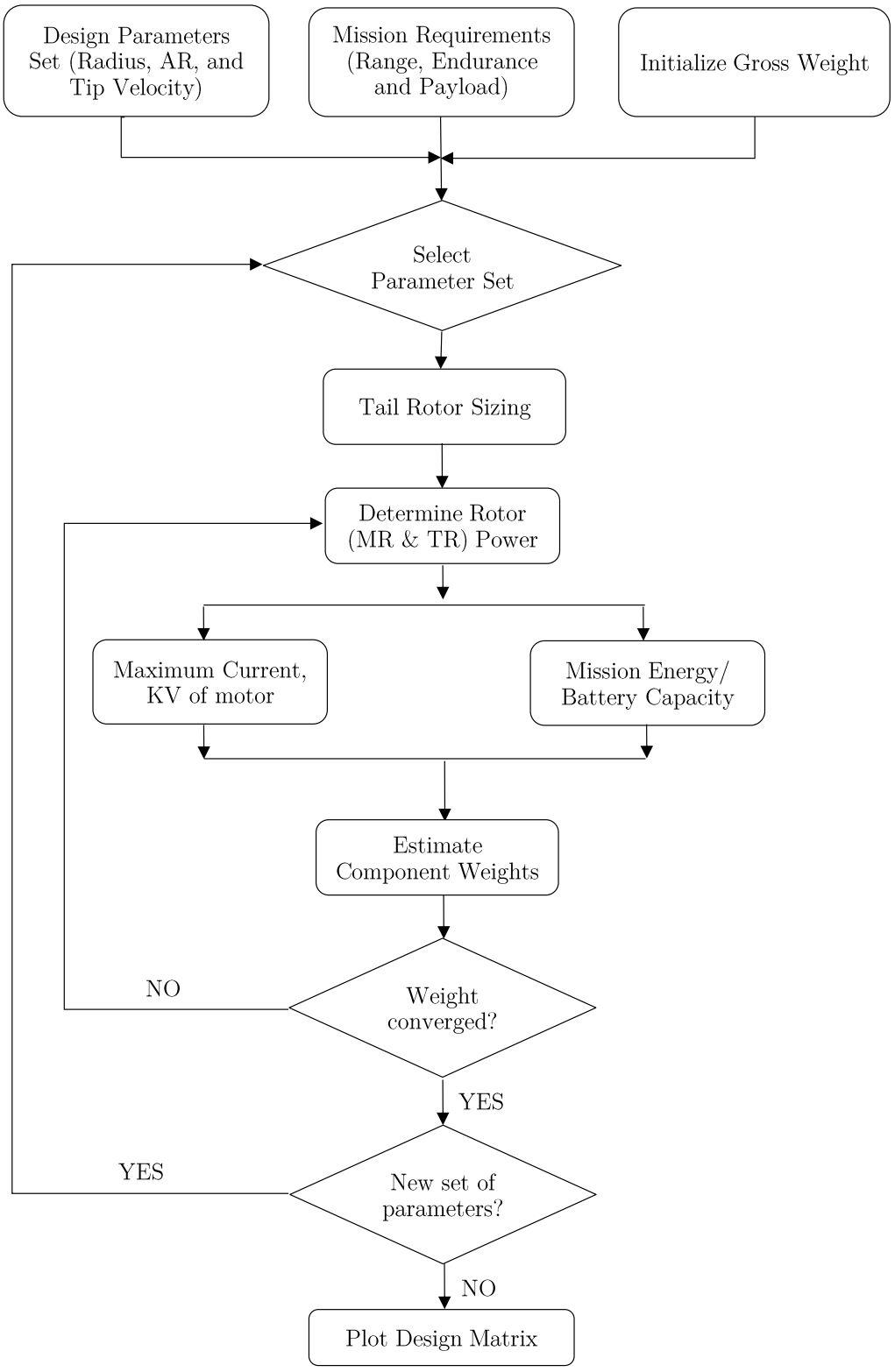

FIGURE 4.2: Design process of a electric powered RWUAV.

the weight of ESC. Other RWUAV components like the main rotor, hub and hinge assembly, landing gear, fuselage, controls, electrical and empennage weight are estimated using the equations given in Section 2.3. From the mission requirements and using momentum theory explained in Section 2.2, the power required by the electric powered RWUAV during forward flight is calculated. The forward flight power and HOGE power along with the endurance and range requirement determines the energy to be stored in the battery. With the mission energy and specific energy density of the Li-ion batteries, the weight of the battery is calculated using Equation 4.1.

All the sub-component weights are summed into a new GTOW and then compared with initial assumed gross weight. If the difference is within the range, then iteration ends, else the assumed weight is replaced by new weight, and component weights are calculated again. This sizing loop goes on until the iteration converges. After the iteration converges for the selected parameter set,the next set is chosen, and the loop continues until all the possible design parameters are studied and plotted.

4.6 Results

The electric powered conventional helicopter is designed for minimum gross weight and minimum energy required to satisfy the mission requirements. The final design should also satisfy the available power constraint of 30hp at 5500 m altitude since the propulsion system is fixed. While minimum gross weight and minimum mission energy are desirable, the vehicle should also be compact. These objective functions and design driving parameters are presented by varying primary design variables.

Figure 4.3 plots the gross weight and mission energy versus the main rotor radius for various tip speed and constant aspect ratio. Aspect ratio is considered as 12. Gross weight and mission energy increase with increasing radius and tip speed. As the tip speed decreases, a bigger main rotor radius is required to generate the hover thrust.

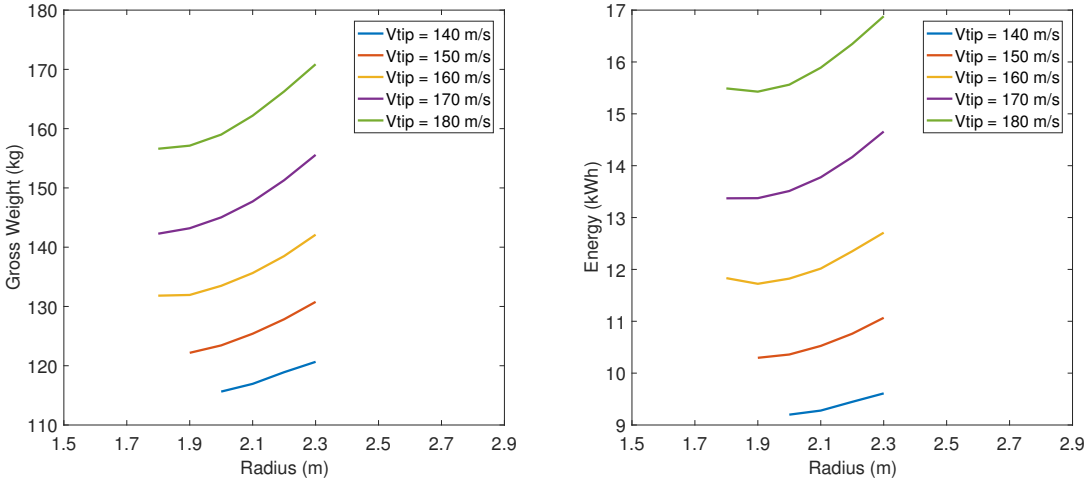

FIGURE 4.3: Variation in gross weight and mission energy for various main rotor radius, tip speed and AR = 12.

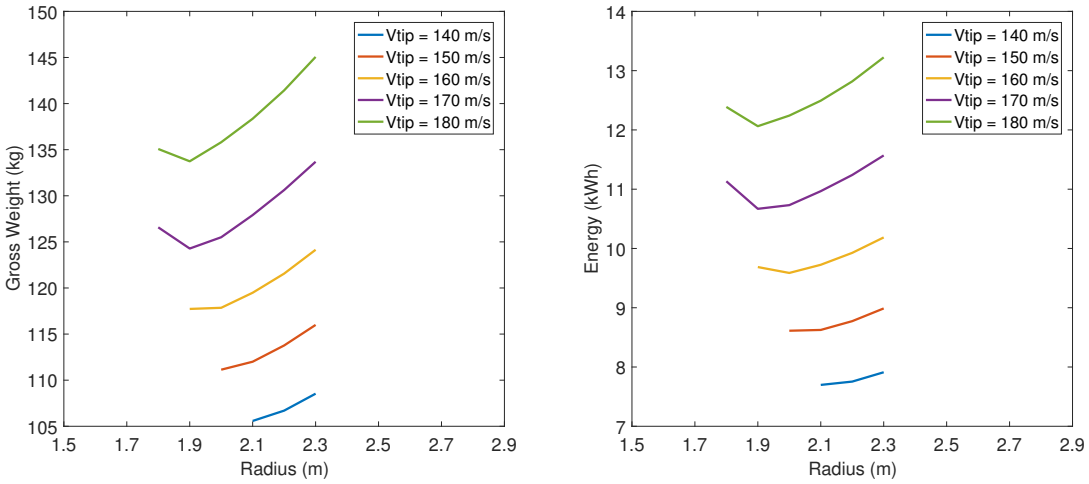

FIGURE 4.4: Variation in gross weight and mission energy for various main rotor radius, tip speed and AR = 16.

Figure 4.4 plots the gross weight and mission energy versus the main rotor radius for various tip speed and constant aspect ratio of 16. It also has the same trends as AR=12, but for lower main rotor radius, there is a sudden increase in gross weight and mission energy. This is because of the increase in main rotor collective pitch angle, thus increasing the hover power and mission energy, as shown in Figures 4.5 and 4.6.

Figures 4.5 and 4.6 shows the variation in hover power and main rotor collective pitch angle for various main rotor radius, tip speed, and aspect ratio. As expected, the hover power

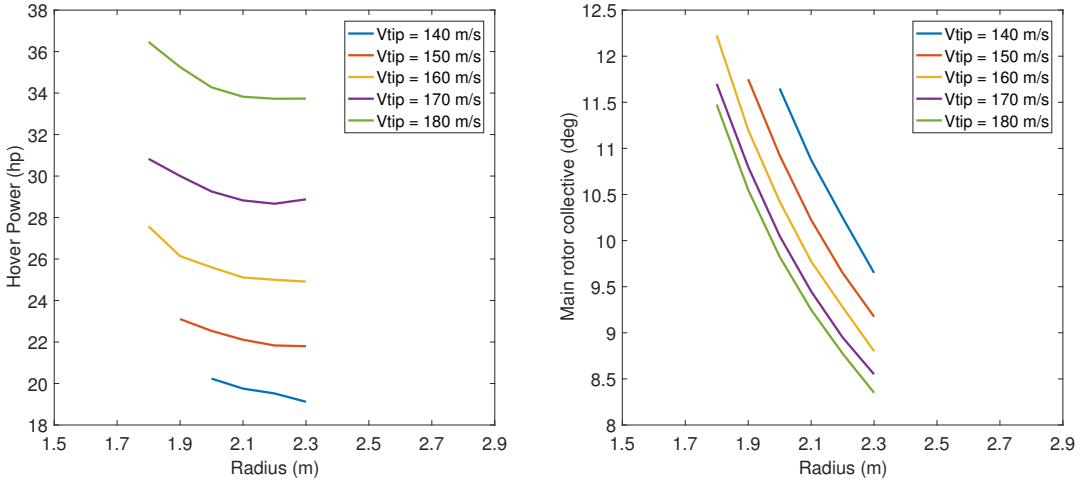

FIGURE 4.5: Variation in hover power and main rotor collective pitch angle for various main rotor radius, tip speed and AR = 12.

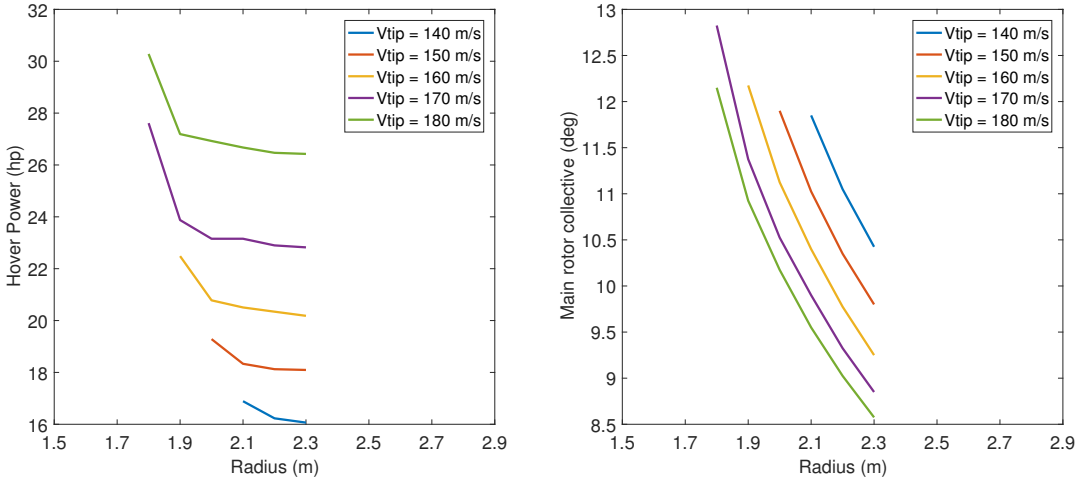

FIGURE 4.6: Variation in hover power and main rotor collective pitch angle for various main rotor radius, tip speed and AR = 16.

reduces for larger main rotor radius. Hover power increases when tip speed is increased for a constant main rotor radius. In contrast, the main rotor collective pitch angle reduces with increasing tip speed for a constant main rotor radius.

There are many possible solutions from this design trade study for electric powered RWUAV. Choosing an optimal solution manually from these options is not possible. For AR=16, the main rotor collective pitch angle is higher than 10deg for most of the solutions except for rotor radius greater than 2.1 m. For AR=12, hover power is higher than

the power available for tip speeds greater than 170 m/s. For AR = 12 and tip speed = 140 m/s, the main rotor collective pitch angle required is more than 10deg. Finally, one preferable design is chosen by neglecting all the nondesirable solutions.

TABLE 4.2: Electric powered RWUAV final design parameters

Parameters	**Values**
Main rotor	
No of Blades, N_b	2
Radius, R_{mr}	2.1 m
Chord, c_{mr}	0.175 m
Aspect Ratio,AR_{mr}	12
Tip speed, $V_{tip_{mr}}$	160 m/s
Disk Loading, DL	96 N/m^2
Solidity, σ_{mr}	0.049
Collective pitch, $\theta_{coll_{mr}}$	9.97 deg
Tail rotor	
No of Blades, N_b	2
Radius, R_{tr}	0.42 m
Chord, c_{tr}	0.070 m
Aspect Ratio,AR_{tr}	6
Blade Pitch	12 deg
Solidity, σ_{tr}	0.106
RPM,	2972

Final design parameters are given in Table 4.2. Main rotor radius is 2.1 m. With an Aspect ratio of 12, main rotor chord value is 0.175m. Disk loading of the current design is 96 N/m^2. With a main rotor radius of 2.1 m and Tip velocity of 160 m/s, the collective pitch angle required to hover is 9.77 deg. The tail rotor is sized as given in Section 2.4. Tail rotor radius is 0.408 m, and with a tip velocity of 167.9 m/s, Tail rotor RPM required to counter the torque generated by the main rotor is 2972.

All the component weight estimates for the final design are given in Table 4.3. Weight estimation formulas given in Sections 2.3 and 3.2 are used to find the weight of the components. For a range of 100km and reserve endurance of 15 minutes, the battery weight required is 45.5 kg. For a payload of 20kg, the gross weight of the final design comes to be 135.6 kg. In fuel powered RWUAV, engine weight and transmission weight takes up

the most of the empty weight whereas, in electric powered RWUAV, battery weight is significantly high comparing other component weights.

TABLE 4.3: Electric powered RWUAV component weight estimates

Parameters	**Values**
Main rotor group	5.66 kg
Main rotor propulsion	9.5 kg
Tail rotor	0.12 kg
Tail rotor propulsion	0.85 kg
Fuselage	10.86 kg
Empennage	1.79 kg
Landing gear	2.03 kg
Controls	6.9 kg
Electrical	6.9 kg
Fixed	25.41 kg
Battery	45.53 kg
Empty	115.6 kg
Payload	20 kg
Gross	135.6 kg

Induced, profile, and parasitic power along with the total power at 5500 m AMSL for the final design is shown in Figure 2.12.

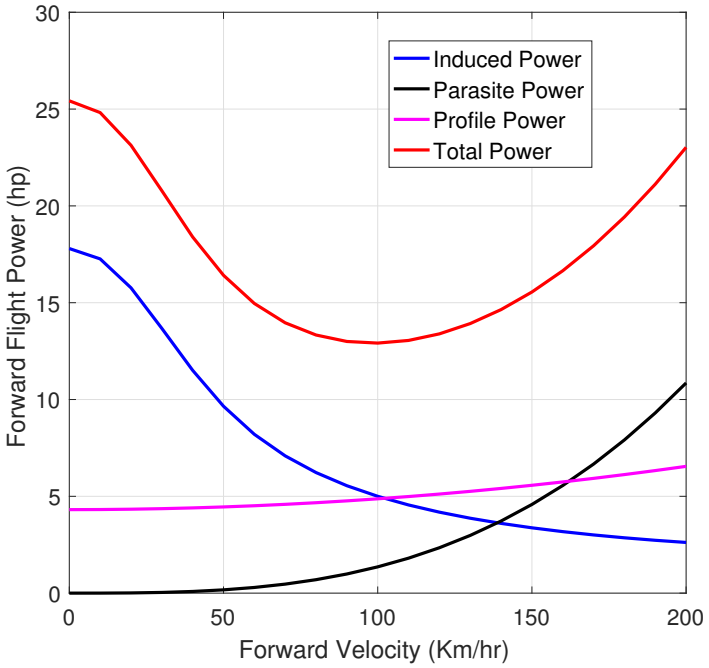

FIGURE 4.7: Forward flight performance of electric powered RWUAV at 5500 m

Total power includes the accessories power and transmission loss. The minimum total power required from Figure 2.12 corresponds to the maximum endurance condition velocity. Performance characteristics of the RWUAV are also given in Table 2.5. Ceiling height of the RWUAV is assumed to be 5500m even though the power required to hover is less than the power available at that height.

TABLE 4.4: Electric powered RWUAV performance characteristics

Parameters	**Values**
HOGE power at 5500 m	25.1 hp
Max Endurance Velocity	100 km/hr
Hover Ceiling	5500 m
Range	100 km
Endurance	1 hr
Mission Energy	12 kWh
Power loading	0.083

Chapter 5

Conclusion

5.1 Summary

The objective of this work is to design a rotary unmanned vehicle that can deliver a payload of 20kg at an altitude of 5500m. Three different rotary vehicle designs were explored that satisfies the mission requirements. The design process has been set up for each vehicle and sized based on the historical data and weight estimation equations from literature. The empirical equations for power calculation usually used in the preliminary analysis are replaced by Blade Element Momentum Theory calculations. Design parameter trade study is explored; this method gives a visual interpretation of changes occurring in the final design when design parameters are changed. Preliminary design of fuel-powered RWUAV is based on the minimum gross weight and minimum hover power at the mission altitude while for multirotors and electric powered RWUAV, the design is based on the minimum gross weight and minimum energy required to complete the mission. Since the objectives of fuel-powered RWUAV are conflicting in nature with the design parameters, multi-objective optimization using genetic algorithm is carried out to find the Pareto optimal solutions. For the other two vehicles, evaluating and plotting the design parameters effect on the objectives allowed us to find an optimal design solution. Performance of the final vehicle

designs was studied and compared with the commercially available vehicles. The final design and performance parameters of the RWUAVs explored are summarized below,

1. Fuel Powered Conventional Helicopter.

    - With a constraint of 30hp power available from a Wankel engine at 5500m AMSL, a conventional helicopter with tail rotor configuration is designed that can deliver a payload of 20kg within a range of 100km.
    - Increasing the main rotor radius decreases the hover power at the same time, it also increases the gross weight.
    - Higher aspect ratio improves the vehicle performance, but very high aspect ratio may require the main rotor to operate at higher collective pitch angles, which is not desirable.
    - For an aspect ratio, higher tip speed requires more profile power while lower tip speed increases the induced power.
    - From a multi-objective optimization using a genetic algorithm for minimum gross weight and hover power, design with main rotor radius of 2.04 m, aspect ratio of 12.92 and tip speed of 167.9 m/s is found to be optimal and satisfies all the mission requirements.
    - Gross take-off weight of the final design converges to 138 kg which requires 26.6 hp power to hover OGE at 5500m AMSL. The designed RWUAV can fly at a cruise velocity of 140 km/hr and has an operational range of 100 km with reserve endurance flight for 15 minutes.

2. Battery Powered Multirotor.

    - While there are many small sized multirotors available in the market, a medium sized multirotor that can deliver a payload of 20kg at an altitude of 5500m AMSL is designed using design trade study.

- Number of rotors and radius of each rotor blade plays a vital role in deciding the performance of the multirotor. For a constant NOR, increasing the radius improves the performance while keeping the radius constant, increasing the NOR improves the performance again. At the same time, it is not true for a higher value of radius where increasing the NOR will increase the gross weight of the multirotor.
- Effect of aspect ratio on the performance is not significant except for very low aspect ratio, but the Voltage of the battery (Number of battery cells connected in series, S) influences the mission performance significantly. Battery weight increases with an increase in voltage, since many cells have to be connected in series. Even though lower voltage is desirable; it is constrained by the operating voltage of the electric motor chosen.
- By evaluating all the design parameters, for a minimum gross weight and minimum mission energy condition final design is chosen as NOR = 12, R = 0.5 m, AR = 6, S = 12 which converges to a gross weight of 71.9 kg and requires mission energy of 2991 Wh.

3. Electric Powered Conventional Helicopter.

- Based on the fuel powered conventional helicopter design, it is assumed that 30 hp power is required for this weight category helicopter to hover at 5000 m AMSL. Hence an electric motor that is capable of generating continuous power of 30 hp is selected, and the RWUAV is designed.
- There are different types of batteries available, all the different configurations based on their chemical configuration is studies and Li-ion batteries with the demonstrated specific energy density of 250 Wh/kg is used as the fuel source in this design. Li-ion batteries are most commonly used in electric vehicles and solar aircraft.

- Higher aspect ratio with the lower main rotor radius requires a large main rotor collective pitch angle, which is not desirable. Increasing the tip speed, reduces the required collective pitch angle but increases the hover power and mission energy of the design.
- Increasing the main rotor radius increases the gross weight significantly, but it also reduces the hover power and main rotor collective pitch angle. Reduction in hover power is not significant at higher rotor radius.
- Finally one superior design is chosen by neglecting all the nondesirable solutions. The final design for the electric powered conventional helicopter is R = 2.1 m, AR = 12, tip speed = 160 m/s which has a gross weight of 135.6 kg and requires a 45 kg of battery to store 12 kWh energy. The HOGE power at an altitude of 5500 m AMSL is 25.1 hp.

Thus design trade study and preliminary design of conventional helicopter and a multirotor are carried out, which will be a cornerstone for the detailed design of these vehicles.

5.2 Future Work

- Sizing formulas and power calculation methods can be replaced with more comprehensive analysis methods in the future. For example, the calculation of hub loads by modeling complete rotor aerodynamics can be done and can be used to calculate the weight of the rotor hub and swashplate.
- In multirotor design, instead of a direct drive system, high torque motor with gearing can be explored for weight reduction.
- In electric powered RWUAV design, instead of choosing an electric motor, propulsion system should also be sized based on the mission requirement.

- Since these RWUAV's operate at high altitude regions, insulation pack for the battery has to be sized, and performance of the battery has to be studied for achieving a better design.

Bibliography

[1] (2014). *Unmanned Vehicles*. The Shephard Press Ltd, England.

[2] A. Krenik, P. W. (2016). Aspects on conceptual and preliminary helicopter design. *Deutscher Luft- und Raumfahrtkongress, Germany*.

[3] Ampatis, C. and Papadopoulos, E. (2014). *Parametric Design and Optimization of Multi-Rotor Aerial Vehicles*, pages 1–25. Springer International Publishing, Cham.

[4] BALCIOGLU, E. (2019). Design and optimization tool for multirotor unmanned aerial vehicles. Master's thesis, Politecnico di Milano, School of Industrial and Information Engineering.

[5] Barth, A., Feil, R., Kondak, K., and Hajek, M. (2014). Conceptual study for an autonomous rotorcraft for extreme altitudes.

[6] Barth, A., Spieß, C., Kondak, K., and Hajek, M. (2018). Design, analysis and flight testing of a high altitude synchropter uav.

[7] Bershadsky, D., Haviland, S., and Johnson, E. (2016). Electric multirotor uav propulsion system sizing for performance prediction and design optimization.

[8] Bouabdallah, S. and Siegwart, R. (2007). *Design and Control of a Miniature Quadrotor*, pages 171–210.

[9] Carl Russel, Jaewoo Jung, G. W. B. G. (2016). Wind tunnel and hover performance test results for multicopter uas vehicles.

[10] Command, A. M. (1974). *ENGINEERING DESIGN HANDBOOK. HELICOPTER ENGINEERING. PART ONE. PRELIMINARY DESIGN.* NTIS, National Technical Iufnatou Service, U. S. DEPARTMENT OF COMMERCE.

[11] Daniel Moëll, J. N. (2008). Vtol uav – a concept study. Master's thesis, Division of Machine Design, Department of Management and Engineering, Sweden.

[12] Du, T., Z. B. M. W. B. B. . S. A. (2016). Computational multicopter design. *ACM Transactions on Graphics.*

[13] Goel, A. (2014). Preliminary design of conventional helicopter using genetic algorithm. Master's thesis, Department of Aerospace Engineering, Indian Institute of Technology, Kanpur.

[14] Hansen, A. C. (1984). An analysis of three approaches to the helicopter preliminary design problem. Master's thesis, Naval Postgraduate School, Monterey, California.

[15] Harrington, R. (1951). Full-scale tunnel investigation of the static thrust performance of a coaxial helicopter rotor. Technical note 2318, NACA.

[16] Kee, S. G. (1983). Guide for conceptual helicopter design. Master's thesis, Naval Postgraduate School, Monterey, California.

[17] Khalid, A. S. (2006). Development and implementation of rotorcraft preliminary design methodology using multidisciplinary design optimization. Master's thesis, Georgia Institute of Technology.

[18] Khromov V, R. O. (2006). Design trends for rotary wing unmanned air vehicles. *25 th International Congress of the Aeronautical Sciences, Germany.*

[19] L. Tartakovsky, V. Baibikov, M. V. (2014). Improvement of wankel engine performance at high altitudes. *3 rd Conference on UAV Propulsion Technologies, Technion, Haifa.*

[20] Leishman, J. G. (2000). *Principles of Helicopter Aerodynamics*. Cambridge University Press, Cambridge, U.K.

[21] M. Emre Gündüz, Adeel Khalid, D. P. S. (2007). Weight estimation using cad in the preliminary rotorcraft design. *33 rd European Rotorcraft Forum, Kazan, Russia*.

[22] Pillai.K, M. (2008). Design and development of an indigenous 55 hp wankel engine. *INCAST 2008-109, Proceedings of the International Conference on Aerospace Science and Technology,Bangalore, India*.

[23] Prouty, R. W. (2002). *Helicopter Performance, Stability, and Control*. Kreiger Publishing Comapny, Malabar, Florida.

[24] Stepniewski, W. . (1983). A comparative study of soviet vs. western helicopters. part 1 - general comparison of designs. Technical report, NASA.

[25] Stepniewski, W. . and Shim, R. A. (1983). A comparative study of soviet vs. western helicopters. part2 - evaluation of weight, maintainability and design aspects of major components. Technical report, NASA.

[26] Venkatesan, S. (2017). A preliminary design of 200kg ruav. Technical report, Department of Aerospace Engineering, Indian Institute of Technology, Kanpur.

[27] Winslow, J., H. V. . C. I. (2017). Design methodology for small-scale unmanned quadrotors. *Journal of Aircraft, 1–9*.

[28] Zhu, X., Guo, Z., and Hou, Z. (2014). Solar-powered airplanes: A historical perspective and future challenges. *Progress in Aerospace Sciences*, 71:36 – 53.